Photorespiration in the context of Rubisco biochemistry, CO_2 diffusion, and metabolism

Florian A. Busch

Research School of Biology and ARC Centre of Excellence for Translational Photosynthesis, Australian National University, Acton ACT 2601, Australia

Author ORCID ID: 0000-0001-6912-0156

* Corresponding author:
Florian Busch
Plant Science Division
Research School of Biology
46 Sullivans Creek Road
The Australian National University
Acton, ACT, 2601
Australia

Tel: +61 2 6125 0123
Email: florian.busch@anu.edu.au

Key words

Rubisco, CO_2 diffusion, mesophyll conductance, photorespiratory C_2 cycle, photosynthetic efficiency, photorespiratory bypass, yield improvement, photosynthesis

Abstract

Photorespiratory metabolism is essential for plants to maintain functional photosynthesis in an oxygen-containing environment. Because the oxygenation reaction of Rubisco is followed by the loss of previously fixed carbon, photorespiration is often considered a wasteful process and considerable efforts are aimed at minimizing the negative impact of photorespiration on the plant's carbon uptake. However, the photorespiratory pathway has also many positive aspects, as it is well integrated within other metabolic processes, such as nitrogen assimilation and C_1 metabolism, and it is important for maintaining the redox balance of the plant. The overall effect of photorespiratory carbon loss on the net CO_2 fixation of the plant is also strongly influenced by the physiology of the leaf related to CO_2 diffusion. This review outlines the distinction between Rubisco oxygenation and photorespiratory CO_2 release as a basis to evaluate the costs and benefits of photorespiration.

Introduction

Photosynthesis is quantitatively the most important biochemical pathway on the planet, by which plants turn sunlight and atmospheric CO_2 into organic biomass. It thereby provides the foundation of most life on Earth. The key enzyme involved in the carboxylation of ribulose 1,5-bisphosphate (RuBP), which drives the assimilation of CO_2 in photosynthetic organisms, is RuBP carboxylase/oxygenase (Rubisco). For every

carboxylation reaction two molecules of 3-phosphoglycerate (3-PGA) are produced that can be metabolized in the Calvin-Benson-Bassham (CBB) cycle to either regenerate RuBP, or to be exported as triose phosphate and become the substrate for most other organic compounds that make up a plant. Almost a century ago, Otto Warburg discovered that the rate of CO_2 assimilation is suppressed by increasing the external oxygen concentration (Warburg, 1920; Nickelsen, 2007). Only much later, and more than a decade after the discovery of Rubisco's capacity to carboxylate its substrate RuBP (Quayle et al., 1954; Weissbach et al., 1954; Mayaudon et al., 1957), it was established that Rubisco is an enzyme that can also react with oxygen to produce one molecule of 2-phosphoglycolate (2-PG) along with one molecule of 3-PGA (Bowes et al., 1971).

The two-carbon molecule 2-PG is a potent inhibitor of several enzymes, including triose phosphate isomerase (Anderson, 1971), sedoheptulose 1,7-bisphosphatase (Flügel et al., 2017), and phosphofructokinase (Kelly and Latzko, 1976) and therefore needs to be metabolized quickly. This is accomplished via the photorespiratory pathway, also known as C_2 pathway or the oxidative photosynthetic carbon cycle. This pathway recovers 75% of the 2-PG carbon by converting it to 3-PGA, which is then fed back into the CBB cycle where it can be used to regenerate RuBP (Berry et al., 1978). The remaining 25% of the carbon is released as CO_2 from photorespiration, meaning 'respiration in the light', as this process is light-dependent. Photorespiration tends to be higher at high temperatures, low CO_2 concentrations and high O_2 concentrations (Sharkey, 1988).

Because of the release of previously fixed CO_2 and the energetic cost involved in metabolizing 2-PG, photorespiration has often been considered wasteful and it has been estimated that decreasing photorespiration could significantly increase food production (Walker et al., 2016). However, considering photorespiration as merely an unwanted side reaction is too simplistic, as the photorespiratory pathway is linked with several other metabolic processes that are essential to the plant. In addition to being connected with the carbon metabolism of the CBB cycle via Rubisco activity and the returned 3-PGA, photorespiration is also involved in nitrogen assimilation (Bloom, 2015; Busch et al., 2018), C_1 metabolism, and amino acid and phospholipid biosynthesis (Hanson and Roje, 2001; Ros et al., 2014). The photorespiratory pathway may also be beneficial through the dissipation of excess energy (Kozaki and Takeba, 1996) and has important implications in balancing the ratio of NADPH and ATP within the cell (Kramer and Evans, 2011).

Photorespiration is the metabolic consequence of the generation of 2-PG via the oxygenation reaction of Rubisco that is recycled via the photorespiratory pathway. As such, the oxygenation reaction is the ultimate cause for photorespiration and, to a large extent, also determines the rate of photorespiratory CO_2 release. Although often conflated with the oxygenation reaction by Rubisco, the CO_2 release from photorespiration is an interrelated, but independent process and the stoichiometry of oxygenation and photorespiration is not fully fixed. Metabolic pathways that drain carbon from the photorespiratory pathway, such as glycine being exported for protein synthesis (Busch et al., 2018) or serine used for C_1 metabolism (Mouillon et al., 1999),

92 will alter the amount of CO_2 released per oxygenation reaction. It is therefore instructive
93 to consider the generation of 2-PG and its metabolism separately. In the following I
94 outline the two sides of photorespiration: (1) the enzymatic properties of Rubisco and
95 aspects of the leaf affecting CO_2 diffusion that determine the generation of 2-PG; and (2)
96 the metabolic context in which photorespiratory recycling of 2-PG occurs. It is these two
97 sides of photorespiration that in combination define photorespiratory CO_2 release and
98 thereby the costs and benefits of photorespiration. I conclude by discussing whether
99 and under which conditions photorespiration might be considered wasteful.
100

101 ## The oxygenation of RuBP by Rubisco

102

103 The rate limiting step of CO_2 fixation in plants is catalyzed by Rubisco, a hexadecameric
104 enzyme that consists of eight large subunits (RbcL) containing the catalytic site and eight
105 small subunits (RbcS) that have some influence over the kinetic properties of Rubisco
106 (Pottier et al., 2018). The key kinetic parameters of Rubisco include the Michaelis-
107 Menten constants for CO_2 (K_c) and O_2 (K_o), and the catalytic turnover speed for
108 carboxylation and oxygenation (k_{cat}^c and k_{cat}^o, respectively, in turnovers per second). The
109 value of k_{cat}^c is only ~2-3 s^{-1} in C_3 plants (Whitney et al., 2011), which is the reason why
110 Rubisco constitutes around 20-30% of soluble leaf protein, but may reach more than
111 50% depending on the growth condition (Makino and Osmond, 1991; Galmés et al.,
112 2014), corresponding to 10-25% of total leaf nitrogen (Onoda et al., 2017; Evans and
113 Clarke, 2019). Its high abundance across all photosynthetic organisms means Rubisco

114 may be the most abundant protein on Earth (Ellis, 1979; Bar-On and Milo, 2019). Both
115 the slow turnover rate and the competitive inhibition by O_2 give Rubisco the reputation
116 of being an inefficient enzyme. However, a recent comparison with chemically related
117 enzymes showed that Rubisco's catalytic performance is not unusual and the perception
118 of it being a particularly sluggish enzyme may be unwarranted (Bathellier et al., 2018).

119 We can mathematically relate the maximum carboxylation capacity (V_{cmax}) and
120 oxygenation capacity (V_{omax}) of Rubisco to the total concentration of enzyme sites (E_t) by
121 defining $V_{cmax} = k_{cat}^{c} E_t$ and $V_{omax} = k_{cat}^{o} E_t$. From these equations we can calculate the ratio
122 of the actual Rubisco carboxylation rate (V_c) relative to its oxygenation rate (V_o) as (Laing
123 et al., 1974):

124 $$\frac{V_c}{V_o} = \frac{V_{cmax}}{K_c} \frac{K_o}{V_{omax}} \frac{C_c}{O}, \quad (1)$$

125 where C_c is the CO_2 concentration and O the O_2 concentration at the Rubisco active site.
126 The ratio of the carboxylation rate to the oxygenation rate when C_c and O are equal is
127 called the relative specificity of Rubisco ($S_{c/o}$) and is given by

128 $$S_{c/o} = \frac{V_{cmax}}{K_c} \frac{K_o}{V_{omax}}. \quad (2)$$

129 $S_{c/o}$ is therefore a property that is determined by the fundamental enzyme kinetics of
130 Rubisco. See Tcherkez (2016) for a detailed discussion of the reaction mechanisms
131 responsible for the partitioning between carboxylation and oxygenation reactions of
132 Rubisco. For given C_c and O, the ratio of the oxygenation to the carboxylation rate is
133 determined by

$$F = \frac{V_o}{V_c} = \left(\frac{1}{S_{c/o}}\right)\frac{O}{C_c}\,. \qquad (3)$$

Eqn. (3) demonstrates that the production of 2-PG through RuBP oxygenation is in a fixed relationship with the production of 3-PGA for any given $S_{c/o}$, C_c, and O. In other words, higher rates of CO_2 fixation are inextricably linked to higher rates of 2-PG production, which then require a higher capacity of 2-PG recycling in the photorespiratory pathway. Consequently, an uncoupling of 3-PGA from 2-PG synthesis can only be achieved by altering $S_{c/o}$, C_c, or O.

Variability of $S_{c/o}$

The $S_{c/o}$ of Rubisco is largely determined by the protein sequence of its subunits and even single amino acid substitutions can impact the kinetic properties of the enzyme. It has been shown that a substitution of Met309 to Ile309 of RbcL turns a C_3-like enzyme with lower k_{cat}^c and higher CO_2 affinity (i.e. lower K_c) into a C_4-like enzyme with higher k_{cat}^c and lower CO_2 affinity (Whitney et al., 2011). Other examples exist where small changes in the protein sequence affected Rubisco kinetic properties, including $S_{c/o}$ (Whitney and Sharwood, 2008) and residues of RbcL have been determined that are under positive selection towards specific kinetic parameters, indicating that RbcL is instrumental in determining the catalytic properties of the enzyme (Kapralov and Filatov, 2007; Kapralov et al., 2010; Galmés et al., 2014).

The role of the small subunit so far is not as well understood, but it has become apparent that it, too, has an impact on the catalytic properties of Rubisco (Spreitzer, 2003; Kapralov et al., 2010). A transformation of the small subunit of *Sorghum bicolor*, a C_4 plant, into the C_3 plant rice has revealed a role for RbcS in controlling catalytic properties (Ishikawa et al., 2011). The transgenic rice plants obtained in these experiments expressing a C_4-type RbcS alongside the native rice RbcL exhibited a higher k_{cat}^{c} and lower $S_{c/o}$ than the non-transgenic rice, making Rubisco's catalytic properties much more C_4-like. Other hybrid enzymes consisting of *Chlamydomonas* RbcL and RbcS from spinach, sunflower, or *Arabidopsis* also produced enzymes with specificities that were intermediate between the wild-type *Chlamydomonas* and the higher plant Rubisco (Genkov et al., 2010). Similarly, a hybrid Rubisco with RbcL from sunflower and RbcS from tobacco showed $S_{c/o}$ values intermediate between sunflower and tobacco (Sharwood et al., 2008). In contrast to RbcL, which is usually encoded by a single-copy gene in the chloroplast, RbcS is a multigene family that encodes several different isoforms in the nuclear genome. The number of rbcS genes can range from as few as 2 in the green alga *Chlamydomonas reinhardtii* to more than 22 in wheat (Spreitzer, 2003). Some of these RbcS variants that are mostly expressed in the mesophyll (M-type) share up to 100% amino acid identity. Another type of RbcS that exists in some plant species and was first found in trichomes (T-type), is distinctly different from the M-type (Pottier et al., 2018). So far, this T-type RbcS has been found in non-photosynthetic tissues such as roots, seeds, fruits, and secretory organs such as trichomes, but appears to be largely absent in photosynthetic tissues (Morita et al., 2016). It can be speculated that this type

176 of RbcS may be important when Rubisco is not being used in the context of the CBB
177 cycle, such as in the fatty acid synthesis during seed development (Schwender et al.,
178 2004). In rice the overexpression of its T-type *RbcS*, *OsRbcS1*, altered the effective
179 catalytic properties of extracted Rubisco (Morita et al., 2014). In these experiments,
180 *OsRbcS1* overexpression increased k_{cat}^{c} and K_c, with a concomitant decrease in $S_{c/o}$,
181 shifting Rubisco's catalytic properties towards those found in C_4 plants. Similar
182 differences were observed when tobacco M-type and T-type *RbcS* genes were expressed
183 in *Chlamydomonas* lacking its own small subunits (Laterre et al., 2017). Small subunits
184 do not have to be as different as M-type and T-type RbcS to confer differences in
185 Rubisco kinetic parameters. Substitutions of single *Chlamydomonas* RbcS residues have
186 been shown to account for decreases in $S_{c/o}$ of up to 8% (Spreitzer et al., 2001).
187 Although direct experimental evidence is lacking to date that the different M-
188 type small subunits within a plant mediate substantial differences in Rubisco kinetic
189 properties *in vivo*, it can be speculated that they do so. Several studies have shown that
190 changes in growth environment, such as temperature (Yoon et al., 2001), light intensity
191 (Wanner and Gruissem, 1991; Dedonder et al., 1993) and light quality (Eilenberg et al.,
192 1998), CO_2 concentration (Cheng et al., 1998), as well as the developmental stage of the
193 plant (Wanner and Gruissem, 1991), result in differential expression of *RbcS* variants.
194 Plants may therefore acclimate to their environment by expressing a Rubisco isoform
195 that is most suitable, e.g. one with high $S_{c/o}$ under conditions where photorespiration
196 would be high, such as high temperatures. An increase in $S_{c/o}$ under high growth
197 temperatures has been experimentally observed in spinach (Yamori et al., 2006),

198 indicating that the acclimation of Rubisco kinetics via expression of different *RbcS*
199 isoforms is at least plausible.

200 Because the half-life of Rubisco inside leaves is in the order of one week
201 (Simpson et al., 1981), any acclimation on the protein level of its kinetic properties
202 cannot happen quickly. However, this does not mean that $S_{c/o}$ necessarily needs to be
203 considered constant over short periods of time. Recent evidence points to the possibility
204 that there may be mechanisms through which Rubisco's kinetic properties can be
205 altered post-translationally. The catalytic site of Rubisco (E) is inactive in its native form
206 (Fig. 1). Its activation requires the binding of non-substrate CO_2 to the Lys201 residue of
207 the active site forming a carbamate (EC) (Sharwood, 2017). This is followed by the
208 binding of Mg^{2+} to create a stable ECM complex, to which the substrate RuBP can bind
209 resulting in the formation of ECMR. The presence of Mg^{2+} and its binding to the catalytic
210 site therefore plays a critical role in the activation of Rubisco. It has been speculated
211 that Mg^{2+} could be replaced by Mn^{2+} inside the chloroplast, which would slightly alter
212 the geometry of the active site (Bloom and Lancaster, 2018). This may differentially
213 change the catalytic properties and thereby favor the oxygenation reaction over the
214 carboxylation reaction. However, so far it is uncertain how much this replacement
215 contributes to the regulation of Rubisco kinetic properties inside the leaf. Experimental
216 evidence of the effect of Mn^{2+} *in vivo* is required, especially since the change in
217 specificity is accompanied by a drastic decrease in the overall catalytic rate (Jordan and
218 Ogren, 1983; Bloom and Kameritsch, 2017).

From an evolutionary perspective, $S_{c/o}$ is fairly constrained within C_3 plants (~85-110 mol mol^{-1} at 25°C)(Hermida-Carrera et al., 2016; Orr et al., 2016), but varies substantially when other organisms such as green and non-green algae or photosynthetic bacteria are included in the comparison, due in part to their different forms of Rubisco (~10 mol mol^{-1} in photosynthetic bacteria, up to ~240 mol mol^{-1} in red algae)(Savir et al., 2010; Young et al., 2016; Flamholz et al., 2019). This variation in specificity is negatively correlated with a variation in k_{cat}^{c}, which has led to the conclusion that there is an unavoidable trade-off between $S_{c/o}$ and k_{cat}^{c}, meaning Rubisco is well optimized to its environmental conditions (Tcherkez et al., 2006; Savir et al., 2010). However, more recent analyses based on data obtained from many more species weaken the apparent inverse relationship between $S_{c/o}$ and k_{cat}^{c} (Galmés et al., 2014; Flamholz et al., 2019), suggesting that photosynthetic organisms have some capacity to adjust V_o relative to V_c without compromising the catalytic rate too much.

As with most other enzymes, the kinetic properties of Rubisco are highly dependent on temperature. With increasing temperatures Rubisco progressively loses its specificity for CO_2 (Badger and Collatz, 1977; Sharwood et al., 2016), meaning that the oxygenation reaction becomes more dominant relative to the carboxylation reaction. This results in generally higher rates of oxygenation and higher losses of carbon from photorespiration at higher leaf temperatures. Surveying a large diversity of species has uncovered a substantial variability in how $S_{c/o}$ is affected by temperature (Hermida-Carrera et al., 2016; Orr et al., 2016; Sharwood et al., 2016). Interestingly, C_3 plants from cool habitats contain Rubiscos that perform better at low temperatures,

241 while Rubiscos from warm-habitat plants perform better at high temperatures (Galmés
242 et al., 2016). Despite these insights into the variability of Rubisco kinetics, the exact
243 molecular bases for what makes $S_{c/o}$ of some Rubiscos more invariant to temperature
244 than others, and which subunit is the main driver for this effect, remain elusive.

245 Overall, $S_{c/o}$ is variable to some degree, both through acclimation to current
246 environmental conditions and adaptation to the plant's habitat. This necessarily impacts
247 V_o and thereby the rate of 2-PG recycling and consequentially the rate of
248 photorespiration. It also means that despite the Rubisco oxygenation reaction
249 potentially being wasteful and unavoidable, plants have some control over how much
250 oxygenation of RuBP they allow to happen. It is interesting to note at this point that
251 plants do not always seem to opt for the highest possible specificity. It is therefore
252 worthwhile to discuss the benefits that plants receive from RuBP
253 oxygenation/photorespiration.

254

255 ***Delivery of CO_2 into the chloroplast***

256

257 Besides $S_{c/o}$, the other important factor determining V_o inside the leaf is O/C_c (Eqn. (3)).
258 Because the O_2 concentration in the atmosphere surrounding the leaf (~ 210,000 µmol
259 mol^{-1}) is much higher than the CO_2 concentration (C_a; ~ 415 µmol mol^{-1}), photosynthetic
260 activity, which releases O_2 at a similar rate as it takes up CO_2, does not substantially alter
261 O. In contrast, in photosynthesizing leaves C_c can vary considerably and reach values
262 much below C_a. This is due to the rate of CO_2 uptake relative to C_a being much larger

than the rate of O_2 release relative to *O*, which according to Fick's law causes a much greater concentration gradient for CO_2 as compared to O_2. We can therefore consider *O* to be a constant in the natural environment and focus here on the variability of C_c.

The CO_2 needed for photosynthesis inside the chloroplast enters the leaf through stomata that tightly regulate the gas exchange between the atmosphere and the inside of the leaf. Thus, stomata impose a resistance to CO_2 diffusion (r_s) that causes the intercellular CO_2 concentration (C_i) to be lower than C_a (Fig. 2a). A similar effect occurs during the diffusion of CO_2 from the intercellular air space to the site of carboxylation in the chloroplast. Here, physical components such as cell walls and membranes impose an additional resistance, termed mesophyll resistance (r_m). According to Fick's law of diffusion, the net CO_2 assimilation rate of a plant (*A*) can be related to changes in the CO_2 concentrations along the diffusive path by making use of these resistances:

$$A = \frac{C_a - C_i}{r_s} = \frac{C_i - C_c}{r_m} \quad (4)$$

Under normal growth conditions, both C_i/C_a and C_c/C_i tend to be around 0.7, resulting in C_c/C_a of about 0.5 (Wong et al., 1978; von Caemmerer and Evans, 1991). This indicates that these resistances have a large impact on C_c and therefore V_o. Stomata respond to a range of environmental signals, such as light intensity and quality, CO_2 concentration, the humidity of the air, and the general water status of the plant (Assmann, 1993; Vavasseur and Raghavendra, 2005; Busch, 2014; Buckley, 2019). In general, stomata open when there is a metabolic need for CO_2 inside the leaf (i.e. the plant is photosynthesizing), and close when the water loss from transpiration exceeds the water availability (Wong et al., 1979; Wong et al., 1985, 1985; Hetherington and Woodward,

2003), making r_s variable on short time scales. Similarly, there is evidence that r_m is also variable, which may be at least in part due to the effective location of (photo)respiratory CO_2 release (Tholen et al., 2012). In the case of chloroplast covering the cell periphery tightly, this forces all (photo)respired CO_2 to diffuse through the chloroplast, effectively resulting in a CO_2 release 'inside the chloroplast' (Fig. 2a). If, however, chloroplast cover is incomplete and the (photo)respiratory CO_2 mixes with the CO_2 coming in from the intercellular air space mostly inside the cytosol, then r_m is an apparent resistance that depends on the diffusive resistance across the cell wall and plasmamembrane (r_{wp}) and the resistance across the chloroplast membrane and stroma (r_{ch}) (Fig. 2b) (for discussion and further explanation see Tholen et al., 2014; Yin and Struik, 2017; Ubierna et al., 2019):

$$r_m = r_{wp} + r_{ch}\frac{V_c}{A} \quad (5)$$

It becomes evident from Eqn. (5) that r_m increases (and the inverse, mesophyll conductance (g_m) decreases) dramatically as A approaches zero (Fig. 2c). This has also been shown experimentally (Busch et al., Accepted). Thus, the location of (photo)respiratory CO_2 release has some impact on C_c, especially when A is low. This idea is exploited by bioengineering approaches that introduce photorespiratory bypasses to relocate photorespiratory CO_2 release from the mitochondria to the chloroplast (Kebeish et al., 2007; Maier et al., 2012; Shen et al., 2019; South et al., 2019). This effectively changes the CO_2 diffusive properties from a "two-resistance" case (Fig. 2b) to a "single-resistance" case (Fig. 2a), which is associated with increases in g_m at low CO_2 concentrations (Fig. 2c).

307 Furthermore, r_m is influenced by anatomical traits, such as cell wall thickness
308 (Ellsworth et al., 2018), chloroplast shape and cover (Busch et al., 2013; Weise et al.,
309 2015), cell density, and the relative amount of intercellular air space (Lehmeier et al.,
310 2017). Mesophyll CO_2 diffusion properties, and consequently the CO_2 concentration
311 inside the chloroplast, therefore are mediated by the 3D anatomy of the mesophyll cells
312 and the leaf as a whole (Earles et al., 2019).

313 Overall, the effective total resistance for CO_2 diffusion (r_t) from C_a to C_c is highly
314 variable with the environment, causing C_c to change according to

315 $$C_c = C_a - Ar_t \,. \tag{6}$$

316 A, in turn, is the difference between the CO_2 taken up by Rubisco and the CO_2 released
317 from photorespiration (F) and mitochondrial respiration (R_d) and can therefore be
318 described by (Farquhar et al., 1980)

319 $$A = V_c - F - R_d \,. \tag{7}$$

320 Here, F relates to V_o through $F = \mathrm{I}\, V_o$, where I is the amount of CO_2 released from
321 photorespiration per oxygenation reaction. The CO_2 concentration, at which the CO_2
322 uptake by Rubisco carboxylation equals CO_2 release from photorespiration is called the
323 CO_2 compensation point in the absence of mitochondrial respiration (Γ^*), and is
324 calculated according to

325 $$\mathrm{G}^* = \frac{\mathrm{I}\, O}{S_{c/o}} \tag{8}$$

326 If the photorespiratory pathway functions as a closed cycle $\mathrm{I} = 0.5$, corresponding to
327 25% of the 2-PG carbon lost as CO_2. Combining Eqn. (7) with Eqns. (3) and (6) we can
328 obtain an expression for V_c

329 $$V_c = \frac{A + R_d}{1 - \mathrm{I\,F}} = \frac{A + R_d}{1 - \frac{\mathrm{I}}{S_{c/o}}\frac{O}{C_c}} = \frac{A + R_d}{1 - \frac{\mathrm{I}}{S_{c/o}}\frac{O}{C_a - Ar_t}} \quad (9)$$

330 and one for *F*

331 $$F = \mathrm{I}\,V_o = \frac{A + R_d}{\frac{1}{\mathrm{I\,F}} - 1} = \frac{A + R_d}{\frac{S_{c/o}}{\mathrm{I}}\frac{C_c}{O} - 1} = \frac{A + R_d}{\frac{S_{c/o}}{\mathrm{I}}\frac{C_a - Ar_t}{O} - 1}\,. \quad (10)$$

332 Eqn. (10) highlights that *F* is not linearly related to *A* because of the additional factor
333 $C_a - Ar_t$. In other words, decreasing *F* by a certain amount does not increase *A* by the
334 same amount, because C_c will change at the same time as a consequence. This can be
335 assessed quantitatively by solving Eqn. (10) for *A*, yielding a quadratic equation in *A* with
336 C_a as the reference CO_2 concentration (see e.g. Farquhar and Busch, 2017). A graphical
337 representation and detailed description of this effect is displayed in Box 1. Most studies
338 to date estimate the impact of photorespiration on *A* by comparing CO_2 assimilation
339 rates with and without photorespiration modelled at a common C_i or C_c, or investigate
340 the rate of photorespiratory CO_2 release at a given internal CO_2 concentration (see e.g.
341 Sharkey, 1988; Valentini et al., 1995; Walker et al., 2016). While these approaches may
342 account for g_m, they disregard that diffusion resistances simultaneously affect both *A*
343 and C_c, and thus ignore that some of the photorespired CO_2 is refixed. Box 1
344 demonstrates that the modelling of *A* has to be coupled to CO_2 diffusion through the
345 stomata and the mesophyll when estimating the effect of photorespiration on net CO_2
346 assimilation rate. The costs of photorespiration on food production as estimated by
347 Walker et al. (2016) is therefore likely an overestimation and should be revisited.

348

Recycling of 2-PG and release of CO_2 by glycine decarboxylation

The primary photorespiratory pathway

Under normal conditions, the oxygenation of RuBP comprises about a quarter of the total use of RuBP by Rubisco, and it can be considerably more under conditions where stomata are substantially impacting CO_2 exchange with the atmosphere. This makes the flux through the photorespiratory pathway the largest biochemical process in plants second only to the flux through the CBB cycle. The 2-PG produced in the oxygenation reaction is dephosphorylated to glycolate by phosphoglycolate phosphatase 1 (PGLP1) in the chloroplast (Fig. 3). Glycolate is exported from the chloroplast by the plastidal glycolate/glycerate translocator 1 (PLGG1), which exchanges chloroplastic glycolate for cytosolic glycerate (Pick et al., 2013). A second transporter, the bile acid sodium symporter BASS6, has recently been implicated in the glycerate-independent export of glycolate, ensuring the balance of glycolate export and glycerate import for varying flux-ratios of these metabolites (South et al., 2017).

In the peroxisome glycolate reacts irreversibly with O_2 and is converted to glyoxylate by glycolate oxidase (GOX), producing H_2O_2 as a byproduct. Catalase (CAT) then decomposes H_2O_2 to water and oxygen. Next, the enzyme glutamate:glyoxylate aminotransferase (GGAT) transaminates glyoxylate to form glycine. A second enzyme that catalyzes the conversion of glyoxylate to glycine is serine:glyoxlate aminotransferase (SGAT), which returns the amino group from the three-carbon branch

371 of the photorespiratory pathway to the two-carbon branch by converting serine into
372 hydroxypyruvate (Fig. 3; Bauwe et al., 2010). The glycine produced is subsequently
373 exported from the peroxisome and taken up by mitochondria. So far, no transporters or
374 channels facilitating the exchange of photorespiratory metabolites between the
375 peroxisomes and the cytosol, or the mitochondrial glycine import and serine export,
376 have been identified (Eisenhut et al., 2013). In the mitochondria glycine is
377 decarboxylated (the source of 'photorespiration') by the multi-enzyme glycine
378 decarboxylase complex (GDC) containing the four cooperating enzymes P-, H-, T-, and L-
379 protein (Douce et al., 2001). This step catalyzes the conversion of the co-factor
380 tetrahydrofolate (THF) to 5,10-methylene-THF (CH_2-THF), which acts as the leaf's
381 currency for activated one-carbon (C_1) units. As a side product, NH_3 is released and
382 NADH generated. CH_2-THF then reacts with a second glycine to form serine in a reaction
383 catalyzed by serine hydroxymethyltransferase 1 (SHMT1). Because the activity of GDC is
384 higher than that of SHMT1, CH_2-THF accumulates in the mitochondria relative to THF
385 (Rebeille et al., 1994).

386 Photorespiratory serine is shuttled back to the peroxisome, where SGAT
387 facilitates the transfer of the amino group to glyoxylate. The resulting hydroxypyruvate
388 is converted to glycerate under the consumption of NADH. This happens either in the
389 peroxisome, facilitated by hydroxypyruvate reductase (HPR1), or in the cytosol by a
390 second hydroxypyruvate reductase (HPR2; Timm et al., 2008). A third enzyme, HPR3,
391 can also react with glyoxylate to form glycolate and operates in the chloroplast (Timm et
392 al., 2011). While the bulk of the flux goes through HPR1 in the peroxisome, the enzymes

in the other compartments allow for a redirection of the flux depending on the availability of NADH in the peroxisome (Timm et al., 2008). As the final step in the photorespiratory pathway, the chloroplastic glycerate kinase (GLYK) phosphorylates glycolate to 3-PGA, which can then enter the CBB cycle. In the case of the photorespiratory pathway operating as a full cycle, three out of four 2-PG carbon atoms will be returned to the CBB cycle and one will be released as CO_2. A detailed description of the enzymatic steps involved in the photorespiratory pathway outlined above can be found in Bauwe (2018).

Reassimilation of NH_3

Glycine decarboxylation in the mitochondria releases NH_3 as a byproduct (Fig. 3). Plants have evolved an efficient mechanism that recaptures and recycles photorespiratory ammonia and it has been estimated that less than 1% is lost to the atmosphere in the process (Mattsson and Schjoerring, 1996). The reassimilation of ammonia is facilitated by two enzymes in the chloroplast, glutamine synthetase (GS2) and ferredoxin-dependent glutamine:oxoglutarate aminotransferase (GOGAT; Coschigano et al., 1998). GS2 converts ammonia and glutamate to glutamine in an ATP-consuming process (Fig. 3). Glutamine then donates an amino group to 2-oxoglutarate (2-OG) to form glutamate in a reaction catalyzed by GOGAT. The glutamate is subsequently transported to the peroxisome, where it is used by GGAT to convert glyoxylate to glycine. The product of this reaction, 2-OG, is returned to the chloroplast to close the cycle.

Interaction with other metabolic pathways

The photorespiratory pathway is essential for all oxygenic phototrophs as a way to metabolize 2-PG and salvage the majority of its carbon. Its importance is demonstrated when the pathway is disrupted by deletion of any of its enzymes, resulting in a photorespiratory phenotype, which may even be lethal (summarized e.g. by Timm and Bauwe, 2013; Eisenhut et al., 2019). The photorespiratory pathway, however, also has other important functions owing to its central position within plant metabolism, and is coupled to the nitrogen-, sulfur-, and C_1- metabolisms by supplying key metabolites and coupled to the TCA cycle and respiration by changing the cell's redox and energy balance (Abadie et al., 2017). For recent reviews on the metabolic integration of the photorespiratory pathway see Hodges et al. (2016) and Obata et al. (2016).

Photorespiration and nitrogen assimilation

The photorespiratory pathway is not only linked to nitrogen assimilation via the reassimilation of photorespiratory ammonia through GS/GOGAT, but also through the reduction and assimilation of new nitrogen, most importantly NO_3^- (Bloom, 2015). Decreasing the flux through the photorespiratory pathway results in decreased rates of NO_3^- uptake and assimilation, demonstrating a clear link between *de novo* nitrogen assimilation and photorespiration (Rachmilevitch et al., 2004; Bloom et al., 2010; Bloom et al., 2012). The photorespiratory pathway is the main biosynthetic pathway for the

amino acids glycine and serine, which are used for many purposes in plant metabolism other than regenerating 3-PGA, such as protein synthesis and as precursors for several other amino acids and phospholipids (Ros et al., 2014). Amino acids produced via the photorespiratory pathway also have a role in stress mitigation as they are key constituents of dehydrins, glutathione, and glycine betaine that increase tolerance to desiccation and prevent damage from reactive oxygen species (Close, 1997; Sakamoto and Murata, 2002; Layton et al., 2010; Noctor et al., 2012). If NO_3^- is available to support *de novo* nitrogen assimilation into glycine and serine, a considerable amount of these amino acids can be diverted from the photorespiratory pathway for other uses, meaning the pathway does not exhibit a fully cyclic nature (Abadie et al., 2016; Busch et al., 2018). Remarkably, because the diverted amino acids contain carbon in addition to nitrogen, the carbon and nitrogen metabolism act synergistically, and this means that photorespiration can increase the overall carbon uptake of a plant despite reducing the efficiency of Rubisco carboxylation (Busch et al., 2018).

Photorespiration and C_1 metabolism

The photorespiratory pathway also interacts with the C_1 metabolism as the main supply of activated C_1 units in the form of CH_2-THF (Li et al., 2003). CH_2-THF has numerous uses throughout the plant's metabolism, such as in the synthesis of nucleic acids, proteins, lipids, chlorophyll, pantothenate, and other methylated molecules (Cossins, 2000; Hanson and Roje, 2001; Gorelova et al., 2017). It is the precursor of several derivatives of THF that are interconverted between 10-formyl-THF (10-CHO-THF), 5,10-methenyl-

459 THF (5,10-CH^+-THF), 5,10-methylene-THF (CH_2-THF), and 5-methyl-THF (5-CH_3-THF),
460 differing by their oxidation state (Fig. 4). C_1 units are drawn from these pools for the
461 synthesis of purines, thymidylate, and pantothenate. The 5-CH_3-THF that is derived from
462 CH_2-THF in a reaction catalyzed by 5,10-methylene-THF reductase (MTHFR) can be used
463 to convert homocysteine to methionine. In addition to protein synthesis, methionine is
464 also involved in the production of S-adenosyl-methionine (SAM), which is used by
465 different methyltransferases (MT) for the methylation of DNA, RNA, proteins,
466 phospholipids, and other substrates (Crider et al., 2012). Both methionine and SAM are
467 assumed to be produced predominantly in the cytosol (Isegawa et al., 1993), supported
468 by the SHMT1-mediated conversion of photorespiratory serine to glycine. The C_1
469 metabolism also plays a major role in the biosynthesis of many secondary products,
470 such as glycine betaine, nicotine, and lignin. It was estimated that the carbon demand in
471 the form of C_1 units for these secondary metabolites can be in the order of 2 mmol C_1
472 units/g dry weight, or about 5% of the total assimilated carbon (Hanson and Roje, 2001).
473
474 ***Photorespiration and sulfur metabolism***
475 The photorespiratory pathway further intersects with, and stimulates, sulfur metabolism
476 (Abadie and Tcherkez, 2019). The synthesis of *O*-acetylserine by serine *O*-
477 acetyltransferase (SAT3) draws from the serine pool in the mitochondria. Reduced sulfur
478 is then incorporated into *O*-acetylserine via *O*-acetylserine (thiol) lyase (OAS-TL) to form
479 cysteine. Cysteine is the primary product of S-assimilation and is required for, among
480 other things, methionine synthesis and glutathione metabolism (Rausch and Wachter,

2005). While the photorespiratory flux supporting this S-metabolism is fairly small compared to that supporting the N- or C_1-metabolism, it should not be considered negligible (Tcherkez and Tea, 2013).

The stoichiometry of CO_2 release per oxygenation reaction

The way photorespiration is embedded with other metabolic pathways shows that numerous biochemical processes rely on the supply of metabolites from the photorespiratory pathway. It is therefore likely that a sizeable proportion of photorespiratory carbon leaves the pathway in the form of glycine, serine, and CH_2-THF and does not get recycled back to 3-PGA. In support of this, the release of CO_2 per oxygenation reaction (I) was shown to be variable and not fixed at 0.5 (Hanson and Peterson, 1985, 1986). In their early attempt to measure the stoichiometry of photorespiratory CO_2 release per oxygenation reaction *in vivo* they determined values ranging from 0.30 to 0.84, depending on environmental conditions such as temperature and light intensity. Since then, other studies have reported a departure of I from 0.5 in mutants that had an impairment in the photorespiratory pathway, such as plants lacking the peroxisomal malate dehydrogenase (PMDH; Cousins et al., 2008), HPR1 (Cousins et al., 2011; Timm et al., 2011), or the thioredoxins THX*h2* or THX*o1* (da Fonseca-Pereira et al., 2019; Reinholdt et al., 2019), and in WT tobacco, wheat, soybean, and Arabidopsis (Walker and Cousins, 2013; Walker et al., 2017). A value of I lower than 0.5 would be expected if carbon is diverted from the photorespiratory pathway as glycine (Busch et

al., 2018). In contrast, the export in the form of CH_2-THF would increase this value towards $I = 1$, because every carbon exported as CH_2-THF releases one carbon as CO_2 in its production by GDC (see Box 2). Based on this, one might expect values of I that are lower than 0.5 in plants that draw more carbon from the photorespiratory pathway in the form of glycine, and values greater than 0.5 in plants that use large amounts of CH_2-THF to synthesize metabolites such as lignin or nicotine. Related to this, Walker et al. (2017) reported that the value of I increases with temperature much more in tobacco than in wheat and soybean. Interestingly, this increase in I corresponds well with an increase in nicotine biosynthesis in tobacco plants exposed to high temperatures (Chen et al., 2016). While the reasons for changes in I *in vivo* are mostly speculative at the moment, further research on the extent of use of photorespiratory carbon for other metabolic processes will undoubtedly lead to significant advances in our understanding of the costs and benefits of photorespiration.

Costs vs. benefits of photorespiration

The interactions of the photorespiratory pathway with other metabolic pathways that draw from photorespiratory metabolites shine a light on which aspects of photorespiration, if any, should be considered wasteful. As outlined above, oxygenation itself is not wasteful *per se* and can provide substantial benefits towards maintaining the redox homeostasis of the cell. The release of photorespiratory CO_2 by GDC should also not be considered a wasteful process as such, as long as it is related to producing

525 metabolites that are needed elsewhere in metabolism, such as glycine, serine, or CH_2-
526 THF. Producing these compounds independently of the photorespiratory pathway would
527 also necessitate reducing equivalents and ATP of similar magnitude – or potentially
528 more – than when going via the photorespiratory pathway. It would also require a
529 steady supply of C_1 compounds that have to be generated with an associated CO_2
530 release. Any cost/benefit analysis therefore has to include an analysis of the possible
531 alternatives. With this in mind, the only portion of photorespiration that we may want
532 to consider 'wasteful' is the flux of 2-PG that actually makes it back to the CBB cycle as
533 3-PGA, as the 25% of carbon lost along the way is not compensated for by other
534 processes (Fig. 3, Box 2). While this 'wasteful' proportion of 2-PG may comprise most of
535 the flux coming from Rubisco's oxygenation reaction under some conditions, such as
536 high temperatures or low CO_2 supply to the chloroplast, it potentially makes up only a
537 small part under other conditions. I am not aware of any direct measurements of
538 *photorespiratory* 3-PGA production relative to 2-PG synthesis, i.e. the effective activities
539 of GLYK relative to PGLP1, that would be useful to evaluate how much of the
540 photorespiratory carbon is put to good use. Indirect evidence that photorespiration is
541 not all wasteful, however, comes from photorespiratory mutant studies. As discussed
542 above, values of I deviating from 0.5 have been previously observed experimentally
543 (Hanson and Peterson, 1985, 1986; Cousins et al., 2008; Cousins et al., 2011; Timm et
544 al., 2011; Walker and Cousins, 2013; da Fonseca-Pereira et al., 2019), which would be
545 expected if carbon is exported from the photorespiratory pathway. These observations
546 hint at that an important role of the photorespiratory pathway is to supply the demand

547 for metabolites for other processes and that it acts as an open pathway rather than a
548 closed cycle when rates of oxygenation are not exceeding this demand. Future studies
549 that aim at quantifying carbon export from the photorespiratory pathway could provide
550 new insights into how leaky the pathway is under varying environments.

551 The interactions of the photorespiratory with other metabolic pathways, as well
552 as the impact that leaf anatomy and physiology have on determining the net effect of
553 photorespiration on carbon balance, make it difficult to assess the impact of these
554 aspects individually on plant performance (see Box 3 for techniques that may be used to
555 quantify photorespiratory carbon fluxes at different points along the pathway). We can,
556 however, gauge the overall short-term effect of photorespiration on carbon uptake,
557 ignoring potential effects due to long-term acclimation. The rate of oxygenation can be
558 instantaneously decreased by experimentally decreasing O (see Eqn. (3)). This allows us
559 to compare A as an integrative parameter for the net cost of photorespiration on CO_2
560 uptake under conditions with and without photorespiration. Despite a substantial
561 proportion of Rubisco activity being used to support the oxygenation reaction, the net
562 effect on A is much smaller for a wide range of environmental conditions (Fig. 5).
563 Especially at C_a of ambient or higher concentrations, the net effect of photorespiration is
564 negligible or even positive. Similarly, at temperatures below about 20°C
565 photorespiration has little or no negative consequences on A in the example shown in
566 Fig. 5. In contrast, photorespiration quickly becomes disadvantageous as leaf
567 temperatures rise above 25°C. Based on these examples, photorespiration appears to be
568 beneficial for the overall carbon uptake for a V_o/V_c of up to approximately 0.25.

569 Photorespiration has further benefits that go beyond the carbon balance of the
570 plant, e.g. due to its contribution to maintaining the redox homeostasis of the cell under
571 abiotic stress conditions such as drought or chilling (Voss et al., 2013). Under certain
572 conditions NADPH and ATP production by the photosynthetic light reactions may exceed
573 their consumption in the CBB cycle. This is likely the case during light induction of
574 photosynthesis under the fluctuating light environments that plants experience e.g. in
575 the understory. Under low light, Rubisco and other CBB cycle enzymes tend to be
576 deactivated and stomata to be relatively closed. If a leaf experiences a sudden increase
577 in light intensity, NADPH and ATP production is induced rapidly (Björkman and Demmig-
578 Adams, 1995), while their consumption is restricted due to slow CBB cycle activation and
579 stomatal opening (Deans et al., 2019; Deans et al., 2019). Under these conditions, the
580 photosynthetic electron transport chain can become over-reduced, causing an increased
581 production of superoxide and other reactive oxygen species, which exacerbates the
582 potential for photodamage (Niyogi, 1999). Photorespiration provides an extra outlet for
583 NADPH and ATP, mitigating the negative effects of excessive light (Kozaki and Takeba,
584 1996; Wingler et al., 2000; Takahashi and Badger, 2011; Eisenhut et al., 2017). While this
585 might come at a carbon cost, the loss in *A* from photorespiration ($D\!A$) is small at least in
586 the case of low stomatal conductance (Box 1), seen e.g. during photosynthetic induction
587 or drought stress. Independent of the magnitude of the actual carbon cost, the energy
588 dissipation aspect of photorespiration increases the resilience of plants under adverse
589 conditions, such as under variable light environments or when limited water availability
590 causes stomata to close.

While photorespiration has certain benefits, it also has costs other than the direct impact on the carbon balance. At a V_o/V_c of 0.33 (an approximate ratio under normal growing conditions, see Fig. 5), one quarter of the nitrogen investment in Rubisco supports the oxygenation reaction, which negatively impacts the photosynthetic nitrogen use efficiency (PNUE) of C_3 plants. Due to higher CO_2 concentrations around Rubisco C_4 plants have much lower rates of oxygenation, which allows them to compromise their Rubisco's $S_{c/o}$ for a higher k^c_{cat}. Thus their nitrogen investment in Rubisco (and other enzymes in the photorespiratory pathway) is much lower than that of C_3 plants, increasing their PNUE (Rotundo and Cipriotti, 2017). It has been shown that an efficient use of nitrogen in C_4 photosynthesis lessens nitrogen cost constraints on molecular sequence evolution (Kelly, 2018). Photorespiration therefore slows both the rate of speciation and extinction in C_3 plants as compared to C_4 plants. Thus, the C_4 photosynthetic pathway may be just as much an adaptation to make the most of the available nitrogen as it is to increase carbon uptake of the plant.

How have plants dealt with photorespiration evolutionarily?

Despite the positive side effects of photorespiration, certain environmental conditions, specifically low CO_2 concentrations, higher temperatures, and conditions inducing stomatal closure, will increase Rubisco oxygenation beyond a flux beneficial for overall plant performance. Plants have evolved several strategies to limit photorespiratory carbon loss, and species with mechanisms that counter photorespiration dominate

environments that are particularly prone to Rubisco oxygenation. It is assumed that a gradual decrease in the atmospheric CO_2:O_2 ratio throughout Earth's history and the associated increase of photorespiration at the cost of carboxylation prompted an adaptation response to these conditions (Moroney et al., 2013). The mechanisms that many plant lineages have evolved can be categorized as either minimizing the rate of oxygenation, resulting in relatively higher carboxylation rates, or minimizing the loss of photorespiratory CO_2 downstream.

Minimizing the rate of oxygenation

The first category includes the carbon concentrating mechanisms (CCMs) of C_4 plants (evolved ~30 Ma; Christin et al., 2011), plants operating a crassulacean acid metabolism (CAM), and the carboxysomes and pyrenoids found in many cyanobacteria and algae, respectively (evolved ~350 Ma; Badger et al., 2002). The common principle by which these CCMs operate includes biochemical and anatomical changes that allow the concentration of CO_2 around Rubisco above ambient levels. This not only decreases the oxygenation rate of Rubisco, but also increases Rubisco's carboxylation rate due to its dependence on the absolute CO_2 concentration following Michaelis-Menten kinetics.

In the C_4 photosynthetic pathway the initial fixation of CO_2 is accomplished in the mesophyll cells by the enzyme phosphoenolpyruvate carboxylase (PEPC) producing the C_4 acid oxaloacetate (OAA). OAA is then converted to malate (or aspartate in some variants of the pathway), which is transported to the bundle sheath cells where Rubisco is located. There the C_4 acid is decarboxylated, producing pyruvate and CO_2, which

635 increases the CO_2 concentration around Rubisco several-fold (Langdale, 2011). This
636 biochemical pathway is usually accompanied by a C_4 Kranz leaf anatomy, which
637 efficiently manages the separation of the C_4- and C_3-pathways (Edwards and
638 Voznesenskaya, 2011). Although the interplay between changes in biochemistry and
639 anatomy is very complex, C_4 photosynthesis is a highly convergent trait that has evolved
640 at least 66 times independently, demonstrating its effectiveness for reducing
641 photorespiration (Sage et al., 2011; Sage et al., 2012). The CAM pathway has similar
642 features to the C_4 pathway, but with a temporal rather than spatial separation of C_3 and
643 C_4 metabolisms (Dodd et al., 2002). In CAM plants CO_2 is initially fixed at night into OAA
644 by PEPC, which is then converted to malate. Malate is stored in the vacuole until
645 daytime, when the conversion back to CO_2 and pyruvate occurs. During the day, the
646 plant's stomata remain closed, resulting in a similar increase in CO_2 concentration
647 around Rubisco as in the bundle sheath cells of C_4 plants. Because the stomata are
648 closed during mid-day when potential rates of transpiration are large, CAM plants can
649 achieve high water-use efficiencies (Szarek and Ting, 1975).

650 CO_2 diffusion in water is several orders of magnitude slower than in air,
651 restricting the ability of plants to access CO_2 for photosynthesis. Aquatic photosynthetic
652 organisms therefore frequently contain CCMs based on encapsulating Rubisco in
653 organelles that restrict outward CO_2 diffusion by a protein shell (in cyanobacterial
654 carboxysomes; Rae et al., 2013) or a starch sheath that may be supplemented by an
655 additional layer of proteins (in algal pyrenoids; Ramazanov et al., 1994). In both cases,
656 CO_2 is converted to bicarbonate in the cytosol before being transported into the

carboxysome or pyrenoid, where it is converted back to CO_2 by the enzyme carbonic anhydrase. This results in an increase in CO_2 concentration around Rubisco, limiting the oxygenation of RuBP.

Despite the existence of a CCM, all these photosynthetic types possess, and require, a fully functioning photorespiratory pathway, though operating at lower fluxes due to decreased Rubisco oxygenation rates that come along with an increased CO_2 concentration around Rubisco (Eisenhut et al., 2008; Zelitch et al., 2009; Levey et al., 2019). Here, the metabolic demand for glycine and serine may at least partially be met through other metabolic pathways, such as the phosphorylated pathway (Igamberdiev and Kleczkowski, 2018). The essential nature of the photorespiratory pathway in C_4 plants, however, might point towards its contribution to providing metabolites for other pathways also in C_4 plants. In any case, increasing the CO_2 concentration inside the cell relaxes the need for a highly substrate-specific Rubisco. Organisms with a CCM usually express a Rubisco that trades off an increased k^c_{cat} for a decreased $S_{c/o}$ (Badger et al., 1998; Sharwood et al., 2016; Heureux et al., 2017; Sharwood, 2017). Non-CCM ways to reduce Rubisco oxygenation include increasing $S_{c/o}$ by lowering the leaf temperature, which can be achieved by decreasing the absorbance of solar radiation or increasing transpiration (Sage, 2013).

Minimizing the loss of photorespiratory carbon

The second category, minimizing the loss of photorespiratory carbon downstream of the production of 2-PG, is a much more boutique approach that has not been as widely

679 adopted in nature. Considered an evolutionary intermediate condition between C_3 and
680 C_4 photosynthesis, some plant species shuttle photorespiratory glycine from the
681 mesophyll to the bundle sheath by restricting GDC to the mitochondria of the bundle
682 sheath cells (Sage et al., 2012). These mitochondria are positioned against the
683 centripetal wall, with chloroplasts covering the cell periphery towards the mesophyll
684 cells (Sage et al., 2013; Sage et al., 2014). This increases the probability of refixation of
685 the photorespiratory CO_2, evidenced by a decrease in the apparent CO_2 compensation
686 point (Sage et al., 2013; Khoshravesh et al., 2016), while at the same time increasing the
687 CO_2 concentration around the population of Rubisco in the bundle sheath.
688 Photorespiratory CO_2 scavenging via this glycine shuttle has been termed C_2
689 photosynthesis, which refers to the number of carbons in the shuttling metabolite
690 glycine (Vogan et al., 2007). The arrangement of chloroplast around the cell periphery as
691 barrier against outward CO_2 diffusion has been shown to be beneficial also in C_3 plants
692 (Busch et al., 2013).

693 Thus, many different approaches exist in nature to combat excessive rates of
694 photorespiration, with the CCMs being the most successful, both in terms of the number
695 of species employing them and their global biomass production. The C_4 photosynthetic
696 pathway stands out, occurring in 3% of the world's plant species and accounting for 23%
697 of the terrestrial primary productivity (Sage et al., 1999; Still et al., 2003). It is a curious
698 observation that the C_4 photosynthetic pathway is, with very few exceptions, limited to
699 herbaceous species. This was hypothesized to be due to constraints associated with the
700 evolutionary history of the C_4 lineages (Sage and Sultmanis, 2016). However, a

contributing factor could be related to the heavy reliance of the arborescent life form on lignin as structural support. Lignin is a large sink for C_1 units (Hanson and Roje, 2001) and one might speculate that this large demand for C_1 units of photorespiratory origin is the reason why the C_4 photosynthetic pathway is largely absent in trees.

Concluding remarks

In summary, predicting the net effect of photorespiration on the CO_2 uptake of plants requires knowledge of the anatomical and physiological properties of the leaf influencing CO_2 diffusion, the kinetic properties of the CO_2-fixing enzyme Rubisco, and the biochemistry of the photorespiratory pathway and how it is connected to other metabolic processes. Each of these aspects influences the rate of photorespiration, resulting in the fact that knowledge of the photorespiratory CO_2 release alone is not sufficient to estimate the carbon cost of photorespiration. In particular, CO_2 diffusive resistances have a large impact on the carbon balance of the photorespiratory pathway. The price a plant has to pay in terms of forgone carbon assimilation is not equal to the carbon lost from photorespiration or the additional carbon that could be assimilated if the RuBP oxygenation reaction were to be replaced by its carboxylation. The actual carbon costs of photorespiration that come into play when V_o/V_c exceeds ~0.25 should be evaluated against the benefits of providing protection against photodamage and helping to balance the ATP to NADPH ratio of the cell, increasing the overall resilience of the plant operating in a variable environment.

Given that the photorespiratory pathway is so well integrated within the plant's metabolism, it may be instructive to view its main purpose as a biosynthetic pathway using a substrate that is available in excess, rather than a pathway for the detoxification of 2-PG. Rubisco can then be considered a dual-functioning enzyme that does not only facilitate the production of primary carbohydrates, but is also the first step in the biosynthesis of several amino acids and compounds relying on the C_1 metabolism. An integrated view of photorespiration within the context of the leaf's biochemical and diffusional properties will ultimately allow us to better target our research efforts towards modifying photorespiration in pursuit of increasing crop productivity.

Acknowledgements

This work was supported by the Australian Government through the Australian Research Council Centre of Excellence for Translational Photosynthesis. I thank Graham Farquhar from The Australian National University for critical feedback on a draft of this manuscript.

Conflict of interest

The author declares no conflict of interest.

Box 1: The effect of diffusion properties on forgone carbon uptake due to photorespiration

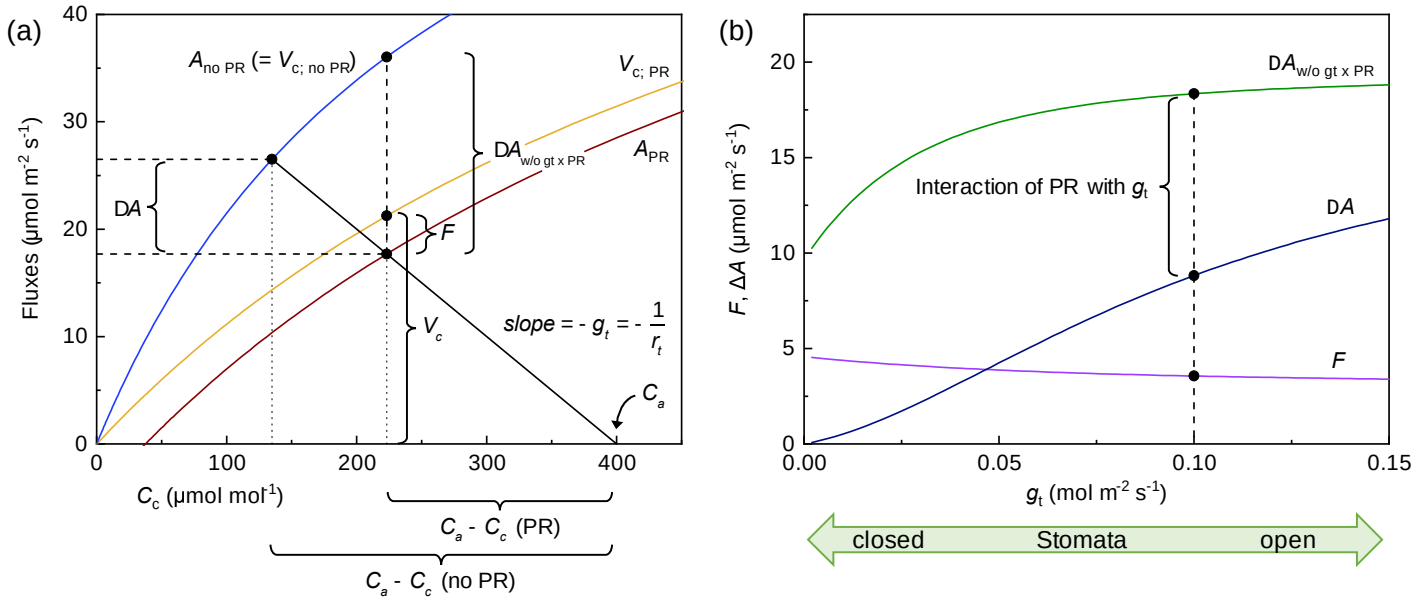

The effect of CO_2 diffusion on carbon uptake forgone due to photorespiration. Panel (a) shows a graphical representation of CO_2 assimilation rates with and without photorespiration. In the simplest case, CO_2 uptake is limited by the rate of Rubisco carboxylation (see Box 2 for the treatment of other biochemical limitations). Then, A can be modelled according to Farquhar et al. (1980) as

$$A = \frac{V_{cmax}\left(C_c - \Gamma^*\right)}{C_c + K_c\left(1 + O/K_o\right)} - R_d \,, \qquad (11)$$

where V_{cmax} is the maximum carboxylation rate of Rubisco, K_c and K_o the Michaelis-Menten constants for CO_2 and O_2. O and C_c are the oxygen and CO_2 concentrations at the site of carboxylation, R_d is the rate of mitochondrial respiration, and Γ^* is the CO_2

compensation point in the absence of R_d, as defined by Eqn. (8). The red line corresponds to A when photorespiration is present, modeled with Eqn. (11) and V_{cmax} = 80 µmol m^{-2} s^{-1}, K_c = 272 µmol mol^{-1}, K_o = 166 mmol mol^{-1} and O = 210 mmol mol^{-1}. Here, R_d was assumed to be zero for simplicity. V_c in response to C_c when photorespiration is present is displayed by a yellow line. Because we ignore R_d in this example, the difference between V_c and A at a given C_c is then equal to F (Eqn. (7)). We can model A for the case of no photorespiration occurring ($A_{no\ PR}$; blue line), which is mathematically equivalent to setting O in Eqn. (11) to zero. Note that this also results in Γ^* being zero (Eqn. (8)). This has the effect of allowing Rubisco to put all of its activity towards the carboxylation reaction (i.e. $A_{no\ PR} = V_c$, as $R_d = 0$). At any given C_c, A_{PR} is lower than $A_{no\ PR}$ by $\Delta A_{w/o\ gt\ x\ PR}$, which is the added effect of Rubisco forgoing carboxylation activity in favor of oxygenation of RuBP, and the loss of carbon from photorespiration. Here, $\Delta A_{w/o\ gt\ x\ PR}$ represents the net effect of the Rubisco oxygenation reaction, if diffusion resistances are ignored.

The line originating at C_c = 400 µmol mol^{-1} and intercepting the A/C_c curve at the chloroplastic CO_2 concentration corresponding to an ambient C_a of 400 µmol mol^{-1} is called the supply function. It represents the decrease in C_c that will occur due to the assimilation of CO_2 by Rubisco (indicated by the drop in CO_2 concentration C_a-C_c (PR)). From Eqn. (6) it follows that the slope of the supply function is $-\frac{1}{r_t}$ (=-g_t). This means that the C_c intersect of the supply function with the A/C_c curve decreases as r_t increases. Assuming r_t is the same under non-photorespiratory conditions, the supply function

intersects with the $A_{no\ PR}$ line at a lower C_c, because the larger CO_2 assimilation rate causes the CO_2 draw-down (C_a-C_c (no PR)) to be larger. Therefore, the net effect of the Rubisco oxygenation reaction being present, if diffusion resistances are considered, is equal to ΔA. ΔA is generally less than $\Delta A_{w/o\ gt\ x\ PR}$, emphasizing that diffusion resistances moderate the negative impact of photorespiration on A.

In a natural environment, C_a can be considered mostly constant, while C_c will vary on short timescales with changes in both CO_2 diffusion properties and the capacity to fix CO_2. Panel (b) displays F and forgone rates of CO_2 assimilation with (ΔA) and without ($\Delta A_{w/o\ gt\ x\ PR}$) considering diffusion resistances as a function of the total conductance to CO_2 diffusion (g_t) at C_a = 400 µmol mol^{-1}. Here, g_t goes towards zero as stomata close – this is equivalent with the supply function in (a) becoming shallower – but it will also vary with varying mesophyll conductance. As stomata close, and thus C_c decreases, F increases moderately. In contrast, ΔA decreases as g_t decreases, and reaches zero when the stomata are fully closed. This underscores, maybe somewhat counterintuitively, that the rate of photorespiratory CO_2 release is not a good measure for the impact that photorespiration has on net CO_2 uptake. Diffusive resistances have a big impact on the absolute amount of carbon uptake forgone due to photorespiratory processes, as demonstrated by $\Delta A_{w/o\ gt\ x\ PR}$ being considerably larger than ΔA.

Box 2: Accounting for carbon export from the photorespiratory pathway when modelling CO_2 uptake

Export of carbon from the photorespiratory pathway will influence how much carbon is assimilated by the plant overall (Busch et al., 2018). In addition, in the case of export of the nitrogen containing photorespiratory metabolites glycine and serine, it will also affect the nitrogen metabolism. Busch et al. (2018) have developed a model that describes net CO_2 uptake when considering carbon export from the photorespiratory pathway in the form of glycine and serine. Here, I provide a more generalized description that also accounts for the export of carbon through the C_1 metabolism (see Fig. 3).

Following Busch et al. (2018) we denote a_G the proportion of 2-PG carbon that is exported from the photorespiratory pathway as glycine and a_S the proportion exported as serine. Similarly, we define a_T as the proportion of 2-PG carbon exported as CH_2-THF. The overall proportion of 2-PG carbon that is exported cannot exceed 1, and therefore the relation $0 \leq a_G + 2a_T + \frac{4}{3}a_S \leq 1$ must hold. Adding up the electron requirement for carbon reduction, photorespiration, and nitrate reduction necessary to supply the nitrogen in the exported glycine and serine (Fig. S1, see Supporting Information), the actual photosynthetic electron transport rate can be calculated as

$$J_a = \left(4 + \left(4 + 8a_G - 4a_T + 4a_S\right)\Phi\right)V_c \,, \qquad (12)$$

where Φ is defined as in Eqn. (3). Eqn. (12) indicates that J_a is both dependent on Φ as well as on the carbon exported from the photorespiratory pathway. The same is true for

816 the rate of ATP consumption, which is equal to $\left(3+\left(3.5-0.5a_G-a_T-2/3a_S\right)F\right)V_c$. If
817 glycine is removed from the photorespiratory pathway, not only is the rate of electron
818 transport used for nitrogen assimilation affected, but it also decreases the amount of
819 CO_2 released per oxygenation reaction (Γ). In contrast, the removal of CH_2-THF from the
820 pathway results in an increase in Γ, because for every carbon removed as CH_2-THF one
821 carbon is lost from glycine decarboxylation as CO_2. The net CO_2 assimilation rate given
822 by Eqn. (7) therefore needs to be parameterized with

823 $$\Gamma = 0.5\left(1-a_G\right)+a_T. \tag{13}$$

824 Equation (13) demonstrates that Γ can be less or greater than 0.5, subject to the
825 magnitudes of a_G and a_T. Thus, *A* is described by

826 $$A = V_c - \left(0.5\left(1-a_G\right)+a_T\right)V_o - R_d\ . \tag{14}$$

827 Depending on the biochemical process limiting CO_2 assimilation, *A* can be described with
828 the minimum of the three rates W_c, W_j, and W_p (Farquhar et al., 1980), which are the
829 carboxylation rates that can be supported under a Rubisco, electron transport or triose
830 phosphate utilization (TPU) limitation, respectively, so that

831 $$A = \min\left\{W_c, W_j, W_p\right\}\left(1-\frac{\Gamma^*}{C_c}\right) - R_d \tag{15}$$

832 where Γ^* is defined as in Eqn. (8). It becomes evident that Γ^* varies with a_G and a_T.
833 When RuBP supply is not limiting the rate of Rubisco carboxylation, W_c is the limiting
834 factor described by

835 $$W_c = \frac{V_{cmax}C_c}{C_c + K_c\left(1+O/K_o\right)}\ . \tag{16}$$

836 If the electron transport rate (*J*) that drives the regeneration of RuBP is the process that
837 limits *A*, W_j is described by

838 $$W_j = \frac{J}{4 + \left(4 + 8a_G - 4a_T + 4a_S\right)F} \quad (17)$$

839 Finally, at high CO_2 concentrations RuBP regeneration may be controlled by the capacity
840 for starch and sucrose synthesis from triose phosphates to regenerate inorganic
841 phosphate for sustained ATP synthesis (Sharkey, 1985; Busch and Sage, 2017). If TPU is
842 limiting the rate of carboxylation, we can write W_p as

843 $$W_p = \frac{3T_p}{1 - 0.5\left(1 + 3a_G + 6a_T + 4a_S\right)F}, \quad (18)$$

844 where T_p is the rate of triose phosphate utilization of the plant. In Eqn. (18) the
845 denominator corresponds to the flux of carbon (scaled by V_c) exported as triose-
846 phosphates. While an attempts have been made to estimate the values of a_G and a_S
847 (Abadie et al., 2016; Busch et al., 2018), so far there is no information available as to the
848 value of a_T.

849 Because carbon can leave the photorespiratory pathway in several locations, the
850 flux of photorespiratory carbon that makes it back to the CBB cycle as 3-PGA is less than
851 half the rate of RuBP oxygenation. We can quantify this flux mathematically, giving a
852 rough indication of the degree of how 'wasteful' photorespiration is in terms of carbon
853 (this, however, ignores the effect of CO_2 diffusion and other beneficial aspects of
854 photorespiration). This gives a flux of photorespiratory CO_2 release that is not linked to
855 supplying metabolites to other metabolic pathways of

$$\text{Carbon 'wasted' by photorespiration} = \left(0.5 - 0.5a_G - a_T - \frac{2}{3}a_S \right) F \quad . \qquad (19)$$

Therefore, carbon is not 'wasted' by photorespiration if V_o does not exceed the metabolic demand for glycine, serine and CH_2-THF, which is the case for $a_G + 2a_T + \frac{4}{3}a_S = 1.$

Box 3: Measuring photorespiration

As outlined in the main text, photorespiration is a multifaceted pathway that is tightly tied in with other metabolic pathways that draw metabolites from the photorespiratory pathway. As a consequence, the carbon flux through the photorespiratory pathway can change along the pathway and therefore may not be accurately represented by the oxygenation reaction of Rubisco or the CO_2 release from GDC. However, much could be learned about the nature of photorespiration and its costs and benefits by combining measurements of fluxes through different parts of the pathway. A range of techniques suitable to probe different aspects of photorespiration has been discussed previously (Sharkey, 1988; Busch, 2013). Other techniques that can be employed in combination to study the interactions of photorespiration with other biochemical pathways are outlined in the following.

Estimation of the rate of Rubisco oxygenation

The rate of Rubisco oxygenation, which is the main source of 2-PG, is largely determined by Rubisco kinetic properties and the CO_2 and O_2 concentrations at the site of carboxylation. While Rubisco kinetic properties can be determined *in vitro*, C_c can be estimated *in vivo* from gas exchange analysis that is coupled with measurements of carbon isotope discrimination (Farquhar et al., 1982; Evans et al., 1986; Busch et al., Accepted) or, with limitations, chlorophyll fluorescence (Epron et al., 1995; Warren, 2006). An alternative strategy for estimating the rate of Rubisco oxygenation involves $^{13}CO_2$ labeling followed by computational flux estimation (Ma et al., 2014, 2017). This "Isotopically Nonstationary Metabolic Flux Analysis" (INST-MFA) has the benefit of not requiring kinetic constants of the involved enzymes and therefore avoids some of the assumptions inherent to the other methods.

Estimation of CO_2 release from GDC

Carbon isotopes can be used in bulk to separate gross fluxes of CO_2 entering the leaf from (photo)respired CO_2 exiting the leaf. The efflux of photorespiratory $^{12}CO_2$ can be measured in a $^{13}CO_2$ atmosphere (Busch et al., 2013; Busch et al., 2017). A related method uses $^{14}CO_2$ to separate the source pools of photorespiration into primary and stored photosynthates, allowing further details of photorespiratory CO_2 release to be obtained (Pärnik and Keerberg, 1995, 2007).

Estimation of glycine export from the photorespiratory pathway

While the rate of glycine synthesis is a useful parameter to know, it does not inform us *per se* how much photorespiratory carbon leaves the photorespiratory pathway as glycine. Abadie et al. (2016) devised a technique based on isotope labelling and metabolome kinetics coupled with isotope ratio mass spectrometry and nuclear magnetic resonance (NMR) analyses to estimate how much photorespiratory glycine accumulates and is not converted to serine. This approach may be used to determine the value of I .

Estimation of the flux through the C_1 metabolism

Our knowledge about the magnitude of the flux through the C_1 metabolism to date is sparse. Attempts to measure the one-carbon fluxes associated with the photorespiratory metabolism in plants have been made using NMR techniques, and it has been shown that the C_1 units needed for serine synthesis originate mostly from photorespiratory carbon (Prabhu et al., 1996). Less is known about the fate of the CH_2-THF produced by GDC. One of the sinks for C_1 units from the folate cycle is the synthesis of methionine. The flux of ^{13}C-label to methionine synthesis has been estimated with a similar NMR approach and been found to be scaled to net CO_2 assimilation (Gauthier et al., 2010; Abadie et al., 2017). Future studies are warranted to elucidate the overall fluxes through the folate cycle.

References

Abadie C, Boex-Fontvieille ERA, Carroll AJ, Tcherkez G (2016) *In vivo* stoichiometry of photorespiratory metabolism. Nature Plants **2:** 15220

Abadie C, Carroll A, Tcherkez G (2017) Interactions between day respiration, photorespiration, and N and S assimilation in leaves. *In* G Tcherkez, J Ghashghaie, eds, Plant Respiration: Metabolic Fluxes and Carbon Balance. Springer International Publishing, Cham, pp 1-18

Abadie C, Tcherkez G (2019) Plant sulphur metabolism is stimulated by photorespiration. Communications Biology **2:** 379

Anderson LE (1971) Chloroplast and cytoplasmic enzymes II. Pea leaf triose phosphate isomerases. Biochimica et Biophysica Acta (BBA) - Enzymology **235:** 237-244

Assmann SM (1993) Signal transduction in guard cells. Annual Review of Cell Biology **9:** 345-375

Badger MR, Andrews TJ, Whitney SM, Ludwig M, Yellowlees DC, Leggat W, Price GD (1998) The diversity and coevolution of Rubisco, plastids, pyrenoids, and chloroplast-based CO_2-concentrating mechanisms in algae. Canadian Journal of Botany **76:** 1052-1071

Badger MR, Collatz GJ (1977) Studies on the kinetic mechanism of ribulose-1,5-bisphosphate carboxylase and oxygenase reactions, with particular reference to the effect of temperature on kinetic parameters. Carnegie Institution Year Book **76:** 355-361

Badger MR, Hanson D, Price GD (2002) Evolution and diversity of CO_2 concentrating mechanisms in cyanobacteria. Functional Plant Biology **29:** 161-173

Bar-On YM, Milo R (2019) The global mass and average rate of rubisco. Proceedings of the National Academy of Sciences **116:** 4738-4743

Bathellier C, Tcherkez G, Lorimer GH, Farquhar GD (2018) Rubisco isn't really so bad. Plant, Cell & Environment **41:** 705-716

Bauwe H (2018) Photorespiration – damage repair pathway of the Calvin–Benson cycle. *In* Annual Plant Reviews online, Vol 50, pp 293-342

Bauwe H, Hagemann M, Fernie AR (2010) Photorespiration: players, partners and origin. Trends in Plant Science **15:** 330-336

Berry JA, Osmond CB, Lorimer GH (1978) Fixation of $^{18}O_2$ during photorespiration. Plant Physiology **62:** 954-967

Björkman O, Demmig-Adams B (1995) Regulation of photosynthetic light energy capture, conversion, and dissipation in leaves of higher plants. *In* E-D Schulze, MM Caldwell, eds, Ecophysiology of Photosynthesis. Springer Berlin Heidelberg, Berlin, Heidelberg, pp 17-47

Bloom AJ (2015) Photorespiration and nitrate assimilation: a major intersection between plant carbon and nitrogen. Photosynthesis Research **123:** 117-128

Bloom AJ, Asensio JSR, Randall L, Rachmilevitch S, Cousins AB, Carlisle EA (2012) CO_2 enrichment inhibits shoot nitrate assimilation in C_3 but not C_4 plants and slows growth under nitrate in C_3 plants. Ecology **93:** 355-367

Bloom AJ, Burger M, Asensio JSR, Cousins AB (2010) Carbon dioxide enrichment inhibits nitrate assimilation in wheat and *Arabidopsis*. Science **328:** 899-903

Bloom AJ, Kameritsch P (2017) Relative association of Rubisco with manganese and magnesium as a regulatory mechanism in plants. Physiologia Plantarum **161:** 545-559

Bloom AJ, Lancaster KM (2018) Manganese binding to Rubisco could drive a photorespiratory pathway that increases the energy efficiency of photosynthesis. Nature Plants **4:** 414-422

Bowes G, Ogren WL, Hageman RH (1971) Phosphoglycolate production catalyzed by ribulose diphosphate carboxylase. Biochemical and Biophysical Research Communications **45:** 716-722

Buckley TN (2019) How do stomata respond to water status? New Phytologist **224:** 21-36

Busch FA (2013) Current methods for estimating the rate of photorespiration in leaves. Plant Biology **15:** 648-655

Busch FA (2014) Opinion: The red-light response of stomatal movement is sensed by the redox state of the photosynthetic electron transport chain. Photosynthesis Research **119:** 131-140

Busch FA, Deans RM, Holloway-Phillips M-M (2017) Estimation of photorespiratory fluxes by gas exchange. *In* AR Fernie, H Bauwe, APM Weber, eds, Photorespiration. Methods in Molecular Biology, Vol 1653. Humana Press, New York, NY, pp 1-15

Busch FA, Holloway-Phillips M-M, Stuart-Williams H, Farquhar GD (Accepted) Revisiting carbon isotope discrimination in C_3 plants: Respiration rules when photosynthesis is low. Nature Plants

Busch FA, Sage RF (2017) The sensitivity of photosynthesis to O_2 and CO_2 concentration identifies strong Rubisco control above the thermal optimum. New Phytologist **213:** 1036-1051

Busch FA, Sage RF, Farquhar GD (2018) Plants increase CO_2 uptake by assimilating nitrogen via the photorespiratory pathway. Nature Plants **4:** 46-54

Busch FA, Sage TL, Cousins AB, Sage RF (2013) C_3 plants enhance rates of photosynthesis by reassimilating photorespired and respired CO_2. Plant, Cell & Environment **36:** 200-212

Chen X, Chen Q, Zhang X, Li R, Jia Y, Ef AA, Jia A, Hu L, Hu X (2016) Hydrogen sulfide mediates nicotine biosynthesis in tobacco (*Nicotiana tabacum*) under high temperature conditions. Plant Physiology and Biochemistry **104:** 174-179

Cheng S-H, Moore Bd, Seemann JR (1998) Effects of short- and long-term elevated CO_2 on the expression of ribulose-1,5-bisphosphate carboxylase/oxygenase genes and carbohydrate accumulation in leaves of *Arabidopsis thaliana* (L.) Heynh. Plant Physiology **116:** 715-723

Christin P-A, Osborne CP, Sage RF, Arakaki M, Edwards EJ (2011) C_4 eudicots are not younger than C_4 monocots. Journal of Experimental Botany **62:** 3171-3181

Close TJ (1997) Dehydrins: A commonalty in the response of plants to dehydration and low temperature. Physiologia Plantarum **100:** 291-296

Coschigano KT, Melo-Oliveira R, Lim J, Coruzzi GM (1998) Arabidopsis *gls* mutants and distinct Fd-GOGAT genes: implications for photorespiration and primary nitrogen assimilation. The Plant Cell **10:** 741-752

Cossins EA (2000) The fascinating world of folate and one-carbon metabolism. Botany **78:** 691

Cousins AB, Pracharoenwattana I, Zhou W, Smith SM, Badger MR (2008) Peroxisomal malate dehydrogenase is not essential for photorespiration in Arabidopsis but its absence causes an increase in the stoichiometry of photorespiratory CO_2 release. Plant Physiology **148:** 786-795

Cousins AB, Walker BJ, Pracharoenwattana I, Smith SM, Badger MR (2011) Peroxisomal hydroxypyruvate reductase is not essential for photorespiration in Arabidopsis but its absence causes an increase in the stoichiometry of photorespiratory CO_2 release. Photosynthesis Research **108:** 91-100

Crider KS, Yang TP, Berry RJ, Bailey LB (2012) Folate and DNA methylation: a review of molecular mechanisms and the evidence for folate's role. Advances in Nutrition **3:** 21-38

da Fonseca-Pereira P, Souza PVL, Hou L-Y, Schwab S, Geigenberger P, Nunes-Nesi A, Timm S, Fernie AR, Thormählen I, Araújo WL, Daloso DM (2019) Thioredoxin *h2* contributes to the redox regulation of mitochondrial photorespiratory metabolism. Plant, Cell & Environment **43:** 188-208

Deans RM, Brodribb TJ, Busch FA, Farquhar GD (2019) Plant water-use strategy mediates stomatal effects on the light induction of photosynthesis. New Phytologist **222:** 382-395

Deans RM, Farquhar GD, Busch FA (2019) Estimating stomatal and biochemical limitations during photosynthetic induction. Plant, Cell & Environment **42:** 3227-3240

Dedonder A, Rethy R, Fredericq H, Van Montagu M, Krebbers E (1993) *Arabidopsis* rbcS genes are differentially regulated by light. Plant Physiology **101:** 801-808

Dodd AN, Borland AM, Haslam RP, Griffiths H, Maxwell K (2002) Crassulacean acid metabolism: plastic, fantastic. Journal of Experimental Botany **53:** 569-580

Douce R, Bourguignon J, Neuburger M, Rébeillé F (2001) The glycine decarboxylase system: a fascinating complex. Trends in Plant Science **6:** 167-176

Earles JM, Buckley TN, Brodersen CR, Busch FA, Cano FJ, Choat B, Evans JR, Farquhar GD, Harwood R, Huynh M, John GP, Miller ML, Rockwell FE, Sack L, Scoffoni C, Struik PC, Wu A, Yin X, Barbour MM (2019) Embracing 3D complexity in leaf carbon-water exchange. Trends in Plant Science **24:** 15-24

Edwards GE, Voznesenskaya EV (2011) C_4 photosynthesis: kranz forms and single-cell C_4 in terrestrial plants. *In* AS Raghavendra, RF Sage, eds, C_4 photosynthesis and related CO_2 concentrating mechanisms. Springer Netherlands, Dordrecht, pp 29-61

Eilenberg H, Hanania U, Stein H, Zilberstein A (1998) Characterization of *rbcS* genes in the fern *Pteris vittata* and their photoregulation. Planta **206:** 204-214

Eisenhut M, Bräutigam A, Timm S, Florian A, Tohge T, Fernie AR, Bauwe H, Weber APM (2017) Photorespiration is crucial for dynamic response of photosynthetic metabolism and stomatal movement to altered CO_2 availability. Molecular Plant **10:** 47-61

Eisenhut M, Pick TR, Bordych C, Weber APM (2013) Towards closing the remaining gaps in photorespiration – the essential but unexplored role of transport proteins. Plant Biology **15:** 676-685

Eisenhut M, Roell M-S, Weber APM (2019) Mechanistic understanding of photorespiration paves the way to a new green revolution. New Phytologist **223:** 1762-1769

Eisenhut M, Ruth W, Haimovich M, Bauwe H, Kaplan A, Hagemann M (2008) The photorespiratory glycolate metabolism is essential for cyanobacteria and might have been conveyed endosymbiontically to plants. Proceedings of the National Academy of Sciences **105:** 17199-17204

Ellis RJ (1979) The most abundant protein in the world. Trends in Biochemical Sciences **4:** 241-244

Ellsworth PV, Ellsworth PZ, Koteyeva NK, Cousins AB (2018) Cell wall properties in *Oryza sativa* influence mesophyll CO_2 conductance. New Phytologist **219:** 66-76

Epron D, Godard D, Cornic G, Genty B (1995) Limitation of net CO_2 assimilation rate by internal resistances to CO_2 transfer in the leaves of two tree species (*Fagus sylvatica* L and *Castanea sativa* Mill). Plant Cell and Environment **18:** 43-51

Evans JR, Clarke VC (2019) The nitrogen cost of photosynthesis. Journal of Experimental Botany **70:** 7-15

Evans JR, Sharkey TD, Berry JA, Farquhar GD (1986) Carbon isotope discrimination measured concurrently with gas-exchange to investigate CO_2 diffusion in leaves of higher plants. Australian Journal of Plant Physiology **13:** 281-292

Farquhar GD, Busch FA (2017) Changes in the chloroplastic CO_2 concentration explain much of the observed Kok effect: a model. New Phytologist **214:** 570-584

Farquhar GD, O'Leary MH, Berry JA (1982) On the relationship between carbon isotope discrimination and the intercellular carbon dioxide concentration in leaves. Australian Journal of Plant Physiology **9:** 121-137

Farquhar GD, von Caemmerer S, Berry JA (1980) A biochemical model of photosynthetic CO_2 assimilation in leaves of C_3 species. Planta **149:** 78-90

Flamholz AI, Prywes N, Moran U, Davidi D, Bar-On YM, Oltrogge LM, Alves R, Savage D, Milo R (2019) Revisiting trade-offs between Rubisco kinetic parameters. Biochemistry **58:** 3365-3376

Flügel F, Timm S, Arrivault S, Florian A, Stitt M, Fernie AR, Bauwe H (2017) The photorespiratory metabolite 2-phosphoglycolate regulates photosynthesis and starch accumulation in Arabidopsis. The Plant Cell **29:** 2537-2551

Galmés J, Hermida-Carrera C, Laanisto L, Niinemets Ü (2016) A compendium of temperature responses of Rubisco kinetic traits: variability among and within

photosynthetic groups and impacts on photosynthesis modeling. Journal of Experimental Botany **67:** 5067-5091

Galmés J, Kapralov MV, Andralojc PJ, Conesa MÀ, Keys AJ, Parry MAJ, Flexas J (2014) Expanding knowledge of the Rubisco kinetics variability in plant species: environmental and evolutionary trends. Plant, Cell & Environment **37:** 1989-2001

Gauthier PPG, Bligny R, Gout E, Mahe A, Nogues S, Hodges M, Tcherkez GGB (2010) In folio isotopic tracing demonstrates that nitrogen assimilation into glutamate is mostly independent from current CO_2 assimilation in illuminated leaves of *Brassica napus*. New Phytologist **185:** 988-999

Genkov T, Meyer M, Griffiths H, Spreitzer RJ (2010) Functional hybrid rubisco enzymes with plant small subunits and algal large subunits: engineered rbcS cDNA for expression in *Chlamydomonas*. Journal of Biological Chemistry **285:** 19833-19841

Gorelova V, Ambach L, Rébeillé F, Stove C, Van Der Straeten D (2017) Folates in plants: research advances and progress in crop biofortification. Frontiers in Chemistry **5:** doi: 10.3389/fchem.2017.00021

Hanson AD, Roje S (2001) One-carbon metabolism in higher plants. Annual Review of Plant Physiology and Plant Molecular Biology **52:** 119-137

Hanson KR, Peterson RB (1985) The stoichiometry of photorespiration during C_3-photosynthesis is not fixed: Evidence from combined physical and stereochemical methods. Archives of Biochemistry and Biophysics **237:** 300-313

Hanson KR, Peterson RB (1986) Regulation of photorespiration in leaves: Evidence that the fraction of ribulose bisphosphate oxygenated is conserved and stoichiometry fluctuates. Archives of Biochemistry and Biophysics **246:** 332-346

Hermida-Carrera C, Kapralov MV, Galmés J (2016) Rubisco catalytic properties and temperature response in crops. Plant Physiology **171:** 2549-2561

Hetherington AM, Woodward FI (2003) The role of stomata in sensing and driving environmental change. Nature **424:** 901-908

Heureux AMC, Young JN, Whitney SM, Eason-Hubbard MR, Lee RBY, Sharwood RE, Rickaby REM (2017) The role of Rubisco kinetics and pyrenoid morphology in shaping the CCM of haptophyte microalgae. Journal of Experimental Botany **68:** 3959-3969

Hodges M, Dellero Y, Keech O, Betti M, Raghavendra AS, Sage R, Zhu X-G, Allen DK, Weber APM (2016) Perspectives for a better understanding of the metabolic integration of photorespiration within a complex plant primary metabolism network. Journal of Experimental Botany **67:** 3015-3026

Igamberdiev AU, Kleczkowski LA (2018) The glycerate and phosphorylated pathways of serine synthesis in plants: the branches of plant glycolysis linking carbon and nitrogen metabolism. Frontiers in Plant Science **9:** doi: 10.3389/fpls.2018.00318

Isegawa Y, Watanabe F, Kitaoka S, Nakano Y (1993) Subcellular distribution of cobalamin-dependent methionine synthase in *Euglena gracilis* z. Phytochemistry **35:** 59-61

Ishikawa C, Hatanaka T, Misoo S, Miyake C, Fukayama H (2011) Functional incorporation of sorghum small subunit increases the catalytic turnover rate of Rubisco in transgenic rice. Plant Physiology **156:** 1603-1611

Jordan DB, Ogren WL (1983) Species variation in kinetic properties of ribulose 1,5-bisphosphate carboxylase/oxygenase. Archives of Biochemistry and Biophysics **227:** 425-433

Kapralov MV, Filatov DA (2007) Widespread positive selection in the photosynthetic Rubisco enzyme. BMC Evolutionary Biology **7:** 73

Kapralov MV, Kubien DS, Andersson I, Filatov DA (2010) Changes in Rubisco kinetics during the evolution of C_4 photosynthesis in *Flaveria* (Asteraceae) are associated with positive selection on genes encoding the enzyme. Molecular Biology and Evolution **28:** 1491-1503

Kebeish R, Niessen M, Thiruveedhi K, Bari R, Hirsch HJ, Rosenkranz R, Stäbler N, Schönfeld B, Kreuzaler F, Peterhänsel C (2007) Chloroplastic photorespiratory bypass increases photosynthesis and biomass production in *Arabidopsis thaliana*. Nature Biotechnology **25:** 593-599

Kelly GJ, Latzko E (1976) Inhibition of spinach-leaf phosphofructokinase by 2-phosphoglycollate. FEBS letters **68:** 55-58

Kelly S (2018) The amount of nitrogen used for photosynthesis modulates molecular evolution in plants. Molecular Biology and Evolution **35:** 1616-1625

Khoshravesh R, Stinson CR, Stata M, Busch FA, Sage RF, Ludwig M, Sage TL (2016) C_3–C_4 intermediacy in grasses: organelle enrichment and distribution, glycine decarboxylase expression, and the rise of C_2 photosynthesis. Journal of Experimental Botany **67:** 3065-3078

Kozaki A, Takeba G (1996) Photorespiration protects C_3 plants from photooxidation. Nature **384:** 557-560

Kramer DM, Evans JR (2011) The Importance of Energy Balance in Improving Photosynthetic Productivity. Plant Physiology **155:** 70-78

Laing WA, Ogren WL, Hageman RH (1974) Regulation of soybean net photosynthetic CO_2 fixation by the interaction of CO_2, O_2, and ribulose 1,5-diphosphate carboxylase. Plant Physiology **54:** 678-685

Langdale JA (2011) C_4 cycles: Past, present, and future research on C_4 photosynthesis. The Plant Cell Online **23:** 3879-3892

Laterre R, Pottier M, Remacle C, Boutry M (2017) Photosynthetic trichomes contain a specific rubisco with a modified pH-dependent activity. Plant Physiology **173:** 2110-2120

Layton BE, Boyd MB, Tripepi MS, Bitonti BM, Dollahon MNR, Balsamo RA (2010) Dehydration-induced expression of a 31-kDa dehydrin in *Polypodium polypodioides* (*Polypodiaceae*) may enable large, reversible deformation of cell walls. American Journal of Botany **97:** 535-544

Lehmeier C, Pajor R, Lundgren MR, Mathers A, Sloan J, Bauch M, Mitchell A, Bellasio C, Green A, Bouyer D, Schnittger A, Sturrock C, Osborne CP, Rolfe S, Mooney S, Fleming AJ (2017) Cell density and airspace patterning in the leaf can be manipulated to increase leaf photosynthetic capacity. The Plant Journal **92:** 981-994

Levey M, Timm S, Mettler-Altmann T, Borghi GL, Koczor M, Arrivault S, Weber APM, Bauwe H, Gowik U, Westhoff P (2019) Efficient 2-phosphoglycolate degradation

is required to maintain carbon assimilation and allocation in the C_4 plant *Flaveria bidentis*. Journal of Experimental Botany **70:** 575-587

Li R, Moore M, King J (2003) Investigating the regulation of one-carbon metabolism in *Arabidopsis thaliana*. Plant and Cell Physiology **44:** 233-241

Ma F, Jazmin LJ, Young JD, Allen DK (2014) Isotopically nonstationary ^{13}C flux analysis of changes in Arabidopsis thaliana leaf metabolism due to high light acclimation. Proceedings of the National Academy of Sciences **111:** 16967-16972

Ma F, Jazmin LJ, Young JD, Allen DK (2017) Isotopically nonstationary metabolic flux analysis (INST-MFA) of photosynthesis and photorespiration in plants. *In* AR Fernie, H Bauwe, APM Weber, eds, Photorespiration. Methods in Molecular Biology, Vol 1653. Humana Press, New York, NY, pp 167-194

Maier A, Fahnenstich H, von Caemmerer S, Engqvist MKM, Weber APM, Fluegge U-I, Maurino VG (2012) Transgenic introduction of a glycolate oxidative cycle into *A. thaliana* chloroplasts leads to growth improvement. Frontiers in Plant Science **3:** doi: 10.3389/fpls.2012.00038

Makino A, Osmond B (1991) Effects of nitrogen nutrition on nitrogen partitioning between chloroplasts and mitochondria in pea and wheat. Plant Physiology **96:** 355-362

Mate CJ, von Caemmerer S, Evans JR, Hudson GS, Andrews TJ (1996) The relationship between CO_2-assimilation rate, Rubisco carbamylation and Rubisco activase content in activase-deficient transgenic tobacco suggests a simple model of activase action. Planta **198:** 604-613

Mattsson M, Schjoerring JK (1996) Ammonia emission from young barley plants: Influence of N source, light/dark cycles and inhibition of glutamine synthetase. Journal of Experimental Botany **47:** 477-484

Mayaudon J, Benson AA, Calvin M (1957) Ribulose-1,5-diphosphate from and CO_2 fixation by *Tetragonia expansa* leaves extract. Biochimica et Biophysica Acta **23:** 342-351

Morita K, Hatanaka T, Misoo S, Fukayama H (2014) Unusual small subunit that is not expressed in photosynthetic cells alters the catalytic properties of rubisco in rice. Plant Physiology **164:** 69-79

Morita K, Hatanaka T, Misoo S, Fukayama H (2016) Identification and expression analysis of non-photosynthetic Rubisco small subunit, *OsRbcS1*-like genes in plants. Plant Gene **8:** 26-31

Moroney J, Jungnick N, DiMario R, Longstreth D (2013) Photorespiration and carbon concentrating mechanisms: two adaptations to high O_2, low CO_2 conditions. Photosynthesis Research **117:** 121-131

Mouillon J-M, Aubert S, Bourguignon J, Gout E, Douce R, Rébeillé F (1999) Glycine and serine catabolism in non-photosynthetic higher plant cells: their role in C1 metabolism. The Plant Journal **20:** 197-205

Nickelsen K (2007) Otto Warburg's first approach to photosynthesis. Photosynthesis Research **92:** 109-120

Niyogi KK (1999) Photoprotection revisited: Genetic and molecular approaches. Annual Review of Plant Physiology and Plant Molecular Biology **50:** 333-359

Noctor G, Mhamdi A, Chaouch S, Han YI, Neukermans J, Marquez-Garcia B, Queval G, Foyer CH (2012) Glutathione in plants: an integrated overview. Plant, Cell & Environment **35:** 454-484

Obata T, Florian A, Timm S, Bauwe H, Fernie AR (2016) On the metabolic interactions of (photo)respiration. Journal of Experimental Botany **67:** 3003-3014

Onoda Y, Wright IJ, Evans JR, Hikosaka K, Kitajima K, Niinemets Ü, Poorter H, Tosens T, Westoby M (2017) Physiological and structural tradeoffs underlying the leaf economics spectrum. New Phytologist **214:** 1447-1463

Orr D, Alcântara A, Kapralov MV, Andralojc J, Carmo-Silva E, Parry MAJ (2016) Surveying Rubisco diversity and temperature response to improve crop photosynthetic efficiency. Plant Physiology **172:** 707-717

Pärnik T, Keerberg O (1995) Decarboxylation of primary and end products of photosynthesis at different oxygen concentrations. Journal of Experimental Botany **46:** 1439-1447

Pärnik T, Keerberg O (2007) Advanced radiogasometric method for the determination of the rates of photorespiratory and respiratory decarboxylations of primary and stored photosynthates under steady-state photosynthesis. Physiologia Plantarum **129:** 34-44

Pick TR, Bräutigam A, Schulz MA, Obata T, Fernie AR, Weber APM (2013) *PLGG1*, a plastidic glycolate glycerate transporter, is required for photorespiration and defines a unique class of metabolite transporters. Proceedings of the National Academy of Sciences **110:** 3185-3190

Pottier M, Gilis D, Boutry M (2018) The hidden face of rubisco. Trends in Plant Science **23:** 382-392

Prabhu V, Chatson KB, Abrams GD, King J (1996) ^{13}C nuclear magnetic resonance detection of interactions of serine hydroxymethyltransferase with C1-tetrahydrofolate synthase and glycine decarboxylase complex activities in *Arabidopsis*. Plant Physiology **112:** 207-216

Quayle JR, Fuller R, Benson AA, Calvin M (1954) Enzymatic carboxylation of ribulose diphosphate. Journal of the American Chemical Society **76:** 3610-3611

Rachmilevitch S, Cousins AB, Bloom AJ (2004) Nitrate assimilation in plant shoots depends on photorespiration. Proceedings of the National Academy of Sciences of the United States of America **101:** 11506-11510

Rae BD, Long BM, Whitehead LF, Förster B, Badger MR, Price GD (2013) Cyanobacterial carboxysomes: microcompartments that facilitate CO_2 fixation. Journal of Molecular Microbiology and Biotechnology **23:** 300-307

Ramazanov Z, Rawat M, Henk MC, Mason CB, Matthews SW, Moroney JV (1994) The induction of the CO_2-concentrating mechanism is correlated with the formation of the starch sheath around the pyrenoid of *Chlamydomonas reinhardtii*. Planta **195:** 210-216

Rausch T, Wachter A (2005) Sulfur metabolism: a versatile platform for launching defence operations. Trends in Plant Science **10:** 503-509

Rebeille F, Neuburger M, Douce R (1994) Interaction between glycine decarboxylase, serine hydroxymethyltransferase and tetrahydrofolate polyglutamates in pea leaf mitochondria. Biochemical Journal **302:** 223-228

Reinholdt O, Schwab S, Zhang Y, Reichheld J-P, Fernie AR, Hagemann M, Timm S (2019) Redox-regulation of photorespiration through mitochondrial thioredoxin o1. Plant Physiology **181:** 442-457

Ros R, Muñoz-Bertomeu J, Krueger S (2014) Serine in plants: biosynthesis, metabolism, and functions. Trends in Plant Science **19:** 564-569

Rotundo JL, Cipriotti PA (2017) Biological limits on nitrogen use for plant photosynthesis: a quantitative revision comparing cultivated and wild species. New Phytologist **214:** 120-131

Sage RF (2013) Photorespiratory compensation: a driver for biological diversity. Plant Biology **15:** 624-638

Sage RF, Christin P-A, Edwards EJ (2011) The C_4 plant lineages of planet Earth. Journal of Experimental Botany **62:** 3155-3169

Sage RF, Khoshravesh R, Sage TL (2014) From proto-Kranz to C_4 Kranz: building the bridge to C_4 photosynthesis. Journal of Experimental Botany **65:** 3341-3356

Sage RF, Li M, Monson RK (1999) The taxonomic distribution of C_4 photosynthesis. *In* RF Sage, RK Monson, eds, C_4 Plant Biology. Academic Press, San Diego, CA, USA, pp 551-584

Sage RF, Sage TL, Kocacinar F (2012) Photorespiration and the evolution of C_4 photosynthesis. Annual Review of Plant Biology **63:** 19-47

Sage RF, Sultmanis S (2016) Why are there no C_4 forests? Journal of Plant Physiology **203:** 55-68

Sage TL, Busch FA, Johnson DC, Friesen PC, Stinson CR, Stata M, Sultmanis S, Rahman BA, Rawsthorne S, Sage RF (2013) Initial events during the evolution of C_4 photosynthesis in C_3 species of *Flaveria*. Plant Physiology **163:** 1266-1276

Sakamoto A, Murata N (2002) The role of glycine betaine in the protection of plants from stress: clues from transgenic plants. Plant, Cell & Environment **25:** 163-171

Savir Y, Noor E, Milo R, Tlusty T (2010) Cross-species analysis traces adaptation of Rubisco toward optimality in a low-dimensional landscape. Proceedings of the National Academy of Sciences **107:** 3475-3480

Schwender J, Goffman F, Ohlrogge JB, Shachar-Hill Y (2004) Rubisco without the Calvin cycle improves the carbon efficiency of developing green seeds. Nature **432:** 779-782

Sharkey TD (1985) O_2-insensitive photosynthesis in C_3 plants - Its occurrence and a possible explanation. Plant Physiology **78:** 71-75

Sharkey TD (1988) Estimating the rate of photorespiration in leaves. Physiologia Plantarum **73:** 147-152

Sharwood RE (2017) Engineering chloroplasts to improve Rubisco catalysis: prospects for translating improvements into food and fiber crops. New Phytologist **213:** 494-510

Sharwood RE, Ghannoum O, Kapralov MV, Gunn LH, Whitney SM (2016) Temperature responses of Rubisco from Paniceae grasses provide opportunities for improving C_3 photosynthesis. Nature Plants **2:** 16186

Sharwood RE, von Caemmerer S, Maliga P, Whitney SM (2008) The catalytic properties of hybrid Rubisco comprising tobacco small and sunflower large subunits mirror the kinetically equivalent source Rubiscos and an support tobacco growth. Plant Physiology **146:** 83-96

Shen B-R, Wang L-M, Lin X-L, Yao Z, Xu H-W, Zhu C-H, Teng H-Y, Cui L-L, Liu EE, Zhang J-J, He Z-H, Peng X-X (2019) Engineering a new chloroplastic photorespiratory bypass to increase photosynthetic efficiency and productivity in rice. Molecular Plant **12:** 199-214

Simpson E, Cooke RJ, Davies DD (1981) Measurement of protein degradation in leaves of *Zea mays* using [^{3}H]acetic anhydride and tritiated water. Plant Physiology **67:** 1214-1219

South PF, Cavanagh AP, Liu HW, Ort DR (2019) Synthetic glycolate metabolism pathways stimulate crop growth and productivity in the field. Science **363:** eaat9077

South PF, Walker BJ, Cavanagh AP, Rolland V, Badger M, Ort DR (2017) Bile Acid Sodium Symporter BASS6 Can Transport Glycolate and Is Involved in Photorespiratory Metabolism in Arabidopsis thaliana. The Plant Cell **29:** 808-823

Spreitzer RJ (2003) Role of the small subunit in ribulose-1,5-bisphosphate carboxylase/oxygenase. Archives of Biochemistry and Biophysics **414:** 141-149

Spreitzer RJ, Esquivel MG, Du Y-C, McLaughlin PD (2001) Alanine-scanning mutagenesis of the small-subunit βA−βB loop of chloroplast ribulose-1,5-bisphosphate carboxylase/oxygenase: substitution at Arg-71 affects thermal stability and CO_2/O_2 specificity. Biochemistry **40:** 5615-5621

Still CJ, Berry JA, Collatz GJ, DeFries RS (2003) Global distribution of C_3 and C_4 vegetation: Carbon cycle implications. Global Biogeochemical Cycles **17:** 1006

Szarek SR, Ting IP (1975) Photosynthetic efficiency of CAM plants in relation to C_3 and C_4 plants. *In*. Springer Netherlands, Dordrecht, pp 289-297

Takahashi S, Badger MR (2011) Photoprotection in plants: a new light on photosystem II damage. Trends in Plant Science **16:** 53-60

Tcherkez G (2016) The mechanism of Rubisco-catalysed oxygenation. Plant, Cell & Environment **39:** 983-997

Tcherkez G, Tea I (2013) $^{32}S/^{34}S$ isotope fractionation in plant sulphur metabolism. New Phytologist **200:** 44-53

Tcherkez GGB, Farquhar GD, Andrews TJ (2006) Despite slow catalysis and confused substrate specificity, all ribulose bisphosphate carboxylases may be nearly perfectly optimized. Proceedings of the National Academy of Sciences **103:** 7246-7251

Tholen D, Éthier G, Genty B (2014) Mesophyll conductance with a twist. Plant, Cell & Environment **37:** 2456-2458

Tholen D, Ethier G, Genty B, Pepin S, Zhu X-G (2012) Variable mesophyll conductance revisited: theoretical background and experimental implications. Plant, Cell & Environment **35:** 2087-2103

Timm S, Bauwe H (2013) The variety of photorespiratory phenotypes – employing the current status for future research directions on photorespiration. Plant Biology **15:** 737-747

Timm S, Florian A, Jahnke K, Nunes-Nesi A, Fernie AR, Bauwe H (2011) The hydroxypyruvate-reducing system in *Arabidopsis*: multiple enzymes for the same end. Plant Physiology **155:** 694-705

Timm S, Nunes-Nesi A, Pärnik T, Morgenthal K, Wienkoop S, Keerberg O, Weckwerth W, Kleczkowski LA, Fernie AR, Bauwe H (2008) A cytosolic pathway for the conversion of hydroxypyruvate to glycerate during photorespiration in *Arabidopsis*. The Plant Cell **20:** 2848-2859

Ubierna N, Cernusak LA, Holloway-Phillips M, Busch FA, Cousins AB, Farquhar GD (2019) Critical review: incorporating the arrangement of mitochondria and chloroplasts into models of photosynthesis and carbon isotope discrimination. Photosynthesis Research **141:** 5-31

Valentini R, Epron D, Deangelis P, Matteucci G, Dreyer E (1995) *In situ* estimation of net CO_2 assimilation, photosynthetic electron flow and photorespiration in Turkey Oak (*Q. cerris* L) leaves: diurnal cycles under different levels of water supply. Plant Cell and Environment **18:** 631-640

Vavasseur A, Raghavendra AS (2005) Guard cell metabolism and CO_2 sensing. New Phytologist **165:** 665-682

Vogan PJ, Frohlich MW, Sage RF (2007) The functional significance of C_3-C_4 intermediate traits in *Heliotropium* L. (Boraginaceae): gas exchange perspectives. Plant Cell and Environment **30:** 1337-1345

von Caemmerer S (2013) Steady-state models of photosynthesis. Plant Cell and Environment **36:** 1617-1630

von Caemmerer S, Evans J (1991) Determination of the average partial pressure of CO_2 in chloroplasts from leaves of several C_3 plants. Functional Plant Biology **18:** 287-305

Voss I, Sunil B, Scheibe R, Raghavendra AS (2013) Emerging concept for the role of photorespiration as an important part of abiotic stress response. Plant Biology **15:** 713-722

Walker BJ, Cousins AB (2013) Influence of temperature on measurements of the CO_2 compensation point: differences between the Laisk and O_2-exchange methods. Journal of Experimental Botany **64:** 1893-1905

Walker BJ, Orr DJ, Carmo-Silva E, Parry MAJ, Bernacchi CJ, Ort DR (2017) Uncertainty in measurements of the photorespiratory CO_2 compensation point and its impact on models of leaf photosynthesis. Photosynthesis Research **132:** 245-255

Walker BJ, VanLoocke A, Bernacchi CJ, Ort DR (2016) The costs of photorespiration to food production now and in the future. Annual Review of Plant Biology **67:** 107-129

Wanner LA, Gruissem W (1991) Expression dynamics of the tomato *rbcS* gene family during development. The Plant Cell **3:** 1289-1303

Warburg O (1920) Über die Geschwindigkeit der photochemischen Kohlensäurezersetzung in lebenden Zellen. II. Biochemische Zeitschrift **103:** 188-217

Warren C (2006) Estimating the internal conductance to CO_2 movement. Functional Plant Biology **33:** 431-442

Weise SE, Carr DJ, Bourke AM, Hanson DT, Swarthout D, Sharkey TD (2015) The *arc* mutants of *Arabidopsis* with fewer large chloroplasts have a lower mesophyll conductance. Photosynthesis Research **124:** 117-126

Weissbach A, Smyrniotis P, Horecker B (1954) Pentose phosphate and CO_2 fixation with spinach extracts. Journal of the American Chemical Society **76:** 3611-3612

Whitney SM, Houtz RL, Alonso H (2011) Advancing our understanding and capacity to engineer nature's CO_2-sequestering enzyme, Rubisco. Plant Physiology **155:** 27-35

Whitney SM, Sharwood RE (2008) Construction of a tobacco master line to improve Rubisco engineering in chloroplasts. Journal of Experimental Botany **59:** 1909-1921

Whitney SM, Sharwood RE, Orr D, White SJ, Alonso H, Galmes J (2011) Isoleucine 309 acts as a C_4 catalytic switch that increases ribulose-1,5-bisphosphate carboxylase/oxygenase (rubisco) carboxylation rate in *Flaveria*. Proceedings of the National Academy of Sciences of the United States of America **108:** 14688-14693

Wingler A, Lea PJ, Quick WP, Leegood RC (2000) Photorespiration: metabolic pathways and their role in stress protection. Philosophical Transactions of the Royal Society B-Biological Sciences **355:** 1517-1529

Wong S-C, Cowan IR, Farquhar GD (1978) Leaf Conductance in Relation to Assimilation in *Eucalyptus pauciflora* Sieb. ex Spreng. Plant Physiology **62:** 670-674

Wong S-C, Cowan IR, Farquhar GD (1985) Leaf conductance in relation to rate of CO_2 assimilation. II. Effects of short-term exposures to different photon flux densities. Plant Physiology **78:** 826-829

Wong S-C, Cowan IR, Farquhar GD (1985) Leaf conductance in relation to rate of CO_2 assimilation. III. Influences of water stress and photoinhibition. Plant Physiology **78:** 830-834

Wong SC, Cowan IR, Farquhar GD (1979) Stomatal conductance correlates with photosynthetic capacity. Nature **282:** 424-426

Yamori W, Suzuki K, Noguchi KO, Nakai M, Terashima I (2006) Effects of Rubisco kinetics and Rubisco activation state on the temperature dependence of the photosynthetic rate in spinach leaves from contrasting growth temperatures. Plant, Cell & Environment **29:** 1659-1670

Yin X, Struik PC (2017) Simple generalisation of a mesophyll resistance model for various intracellular arrangements of chloroplasts and mitochondria in C_3 leaves. Photosynthesis Research **132:** 211-220

Yoon M, Putterill JJ, Ross GS, Laing WA (2001) Determination of the relative expression levels of Rubisco small subunit genes in *Arabidopsis* by rapid amplification of cDNA ends. Analytical Biochemistry **291:** 237-244

Young JN, Heureux AMC, Sharwood RE, Rickaby REM, Morel FMM, Whitney SM (2016) Large variation in the Rubisco kinetics of diatoms reveals diversity among their carbon-concentrating mechanisms. Journal of Experimental Botany **67:** 3445-3456

Zelitch I, Schultes NP, Peterson RB, Brown P, Brutnell TP (2009) High glycolate oxidase activity is required for survival of maize in normal air. Plant Physiology **149:** 195-204

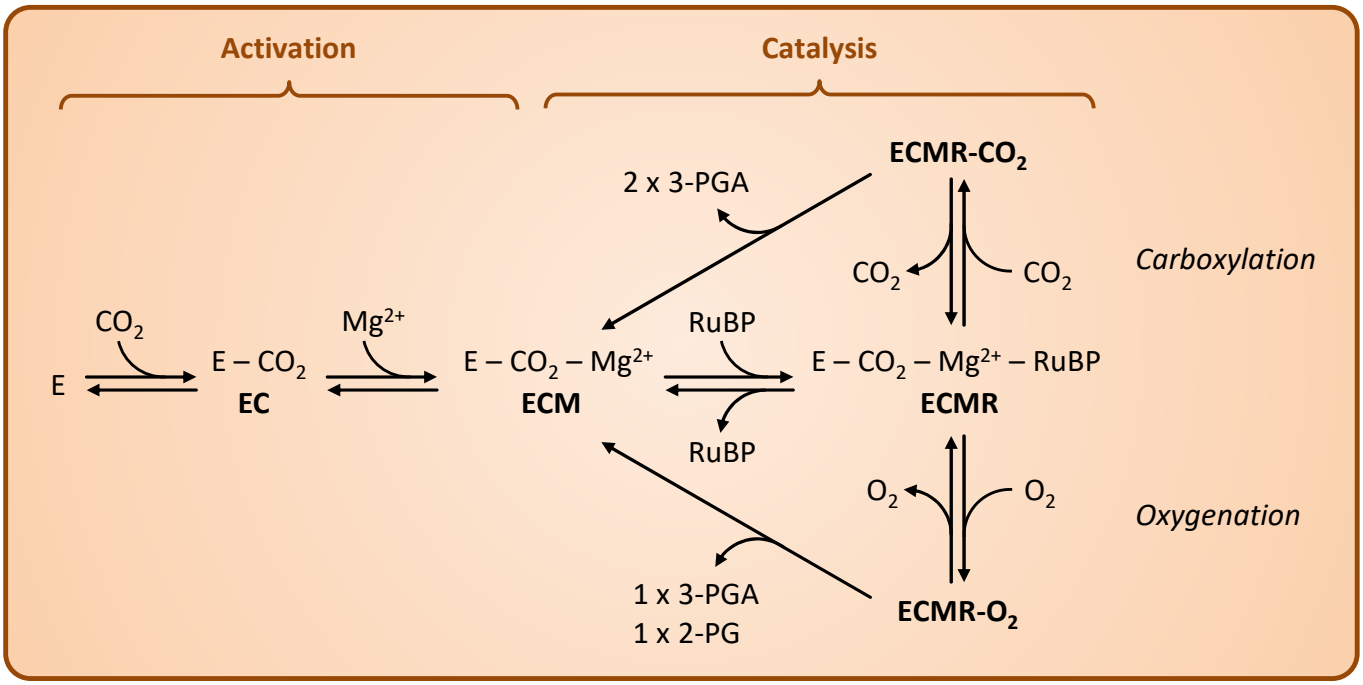

1443

1444 **Figure 1**

1445 **Activation and catalysis sequence of Rubisco.** Inactive Rubisco enzyme (E) becomes

1446 carbamated by the binding of non-substrate CO_2 (EC) followed by the activation through

1447 the binding of Mg^{2+} (ECM). The activated Rubisco binds ribulose-1,5-bisphosphate

1448 (RuBP) forming the ECMR complex, which can then react either with CO_2 in a

1449 carboxylation reaction producing two molecules of 3-phosphoglycerate (3-PGA), or with

1450 O_2 in an oxygenation reaction producing one molecule of 3-PGA and one of 2-

1451 phosphoglycolate (2-PG). Figure adapted from Mate et al. (1996).

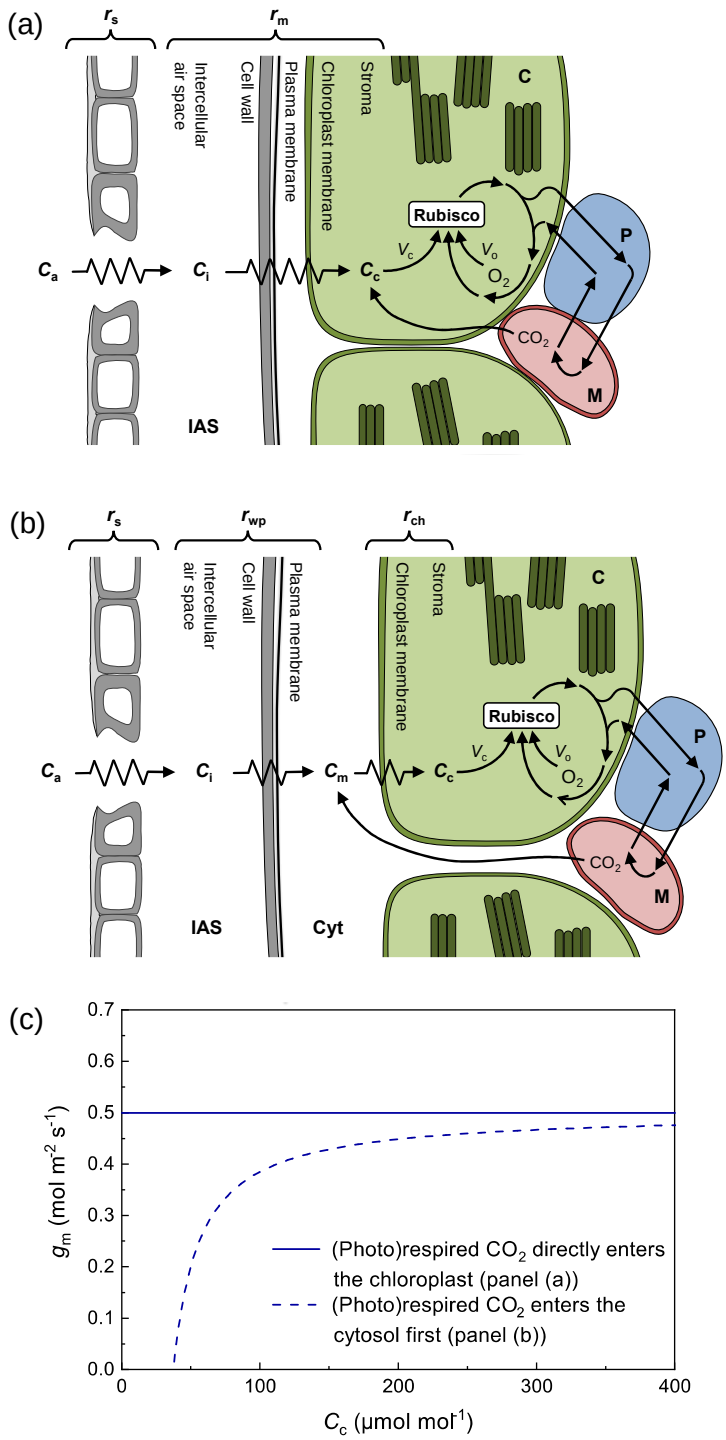

Figure 2

Resistances to CO_2 diffusion inside the leaf affecting the CO_2 concentration around Rubisco. The photorespiratory pathway involves the subcellular compartments chloroplasts (C), peroxisomes (P) and mitochondria (M). (a) (Photo)respired CO_2 is

1456 effectively released inside the chloroplast. This is the case if chloroplasts fully cover the
1457 cell periphery and the mitochondria are located towards the inside of the cell. It is also
1458 achieved in plants bioengineered to release photorespiratory CO_2 directly inside the
1459 chloroplast. The resistances imposed by stomata (r_s) and the mesophyll (r_m), which
1460 includes the cell wall and membranes, cause a progressive decline in CO_2 concentrations
1461 from the ambient air (C_a) to the intercellular air space (IAS; C_i) and the chloroplast (C_c).
1462 (b) If (photo)respired CO_2 mixes with the CO_2 coming from the IAS inside the cytosol,
1463 which is the case e.g. when chloroplasts are further apart, or mitochondria are located
1464 between the cell wall and the chloroplasts, then r_m becomes an apparent resistance that
1465 varies with the amount of CO_2 released from (photo)respiration (see text for further
1466 information). In this case, r_m has to be separated into a cell wall and plasmalemma
1467 component (r_{wp}) and a chloroplast envelope and stromal component (r_{ch}). (c) The CO_2
1468 response of the mesophyll conductance (g_m) to CO_2 diffusion for the two scenarios
1469 outlined in panels (a) and (b), modelled for equal contribution of r_{ch} and r_{wp}. Note that
1470 when (photo)respiratory CO_2 enters the cytosol first, the apparent value of g_m tends to
1471 zero when the compensation point ($A = 0$) is approached. Panels (a) and (b) adapted
1472 from von Caemmerer (2013)
1473

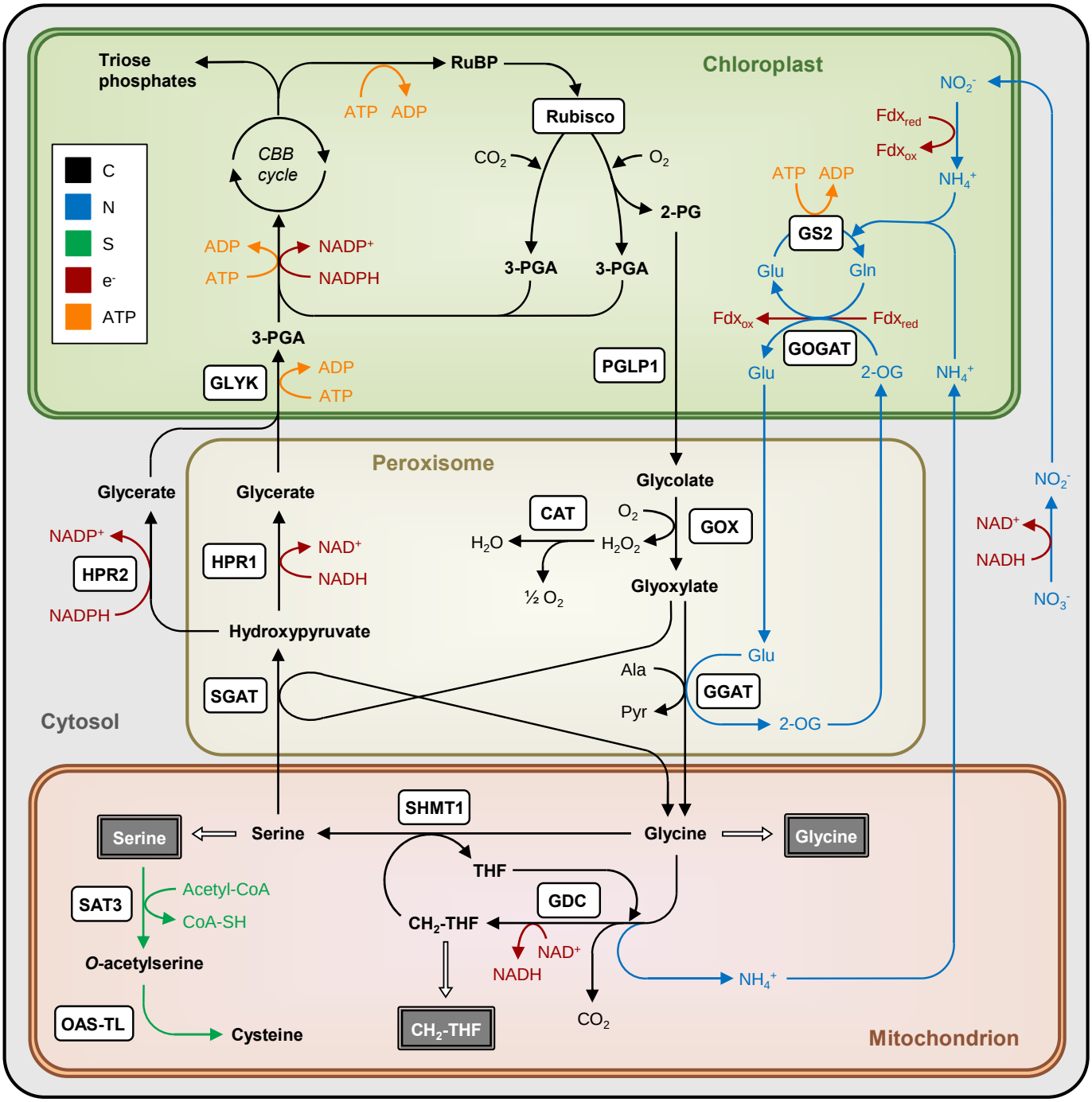

1474

1475 **Figure 3**

1476 **Schematic of the photorespiratory metabolism.** The movement of carbon along the

1477 photorespiratory pathway (black arrows) and the metabolites involved (bold font) are

1478 shown in the context of the nitrogen (blue) and sulfur metabolism (green). Redox

reactions involving NAD, NADP, or ferredoxin (Fdx) are shown in red and ATP consuming processes in orange. Photorespiratory carbon leaves the pathway as CO_2 during the glycine decarboxylation step or is returned to the CBB cycle as 3-PGA. Carbon may also be exported from the photorespiratory pathway (white arrows) in the form of the amino acids glycine and serine, or as CH_2-THF, which supplies one-carbon (C_1) units to the C_1 metabolism (grey boxes). The amount of exported carbon influences how much photorespiratory carbon is returned to the CBB cycle. 2-PG, 2-phosphoglycolate; 3-PGA, 3-phosphoglycerate; 2-OG, 2-oxoglutarate; PGLP1, phosphoglycolate phosphatase 1; GOX, glycolate oxidase; CAT, catalase; GGAT, glutamate:glyoxylate aminotransferase; SGAT, serine:glyoxylate aminotransferase; GDC, glycine decarboxylase complex; SHMT1, serine hydroxymethyltransferase 1; HPR1, hydroxypyruvate reductase 1; HPR2, hydroxypyruvate reductase 2; GLYK, glycerate kinase; GS2, glutamine synthetase; GOGAT, glutamine:oxoglutarate aminotransferase; SAT3, serine *O*-acetyltransferase; OAS-TL, *O*-acetylserine (thiol) lyase (Figure adapted from Bauwe et al., 2010; Eisenhut et al., 2019).

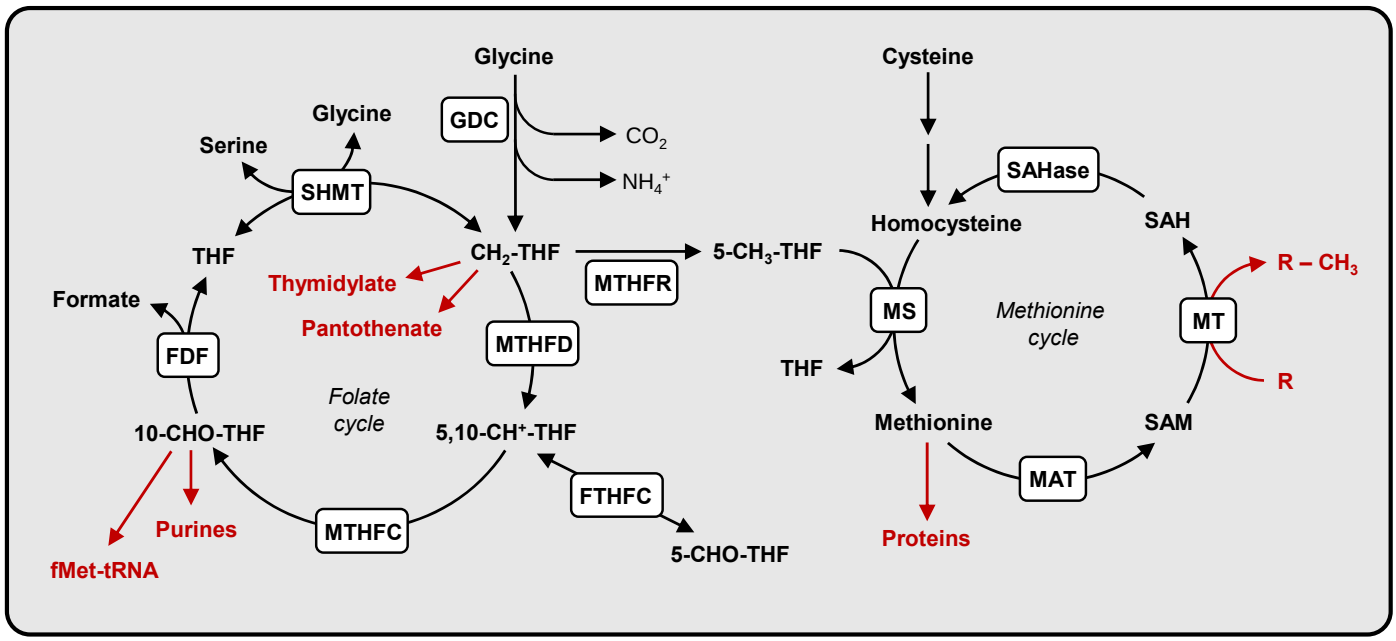

1495

1496 **Figure 4**

1497 **Metabolic uses of C_1 units outside the photorespiratory pathway.** CH_2-THF exported

1498 from the photorespiratory pathway is the precursor for several derivatives of THF that

1499 can be interconverted and their C_1 units used for the biosynthesis of a wide range of

1500 primary and secondary metabolites (shown in red). A major sink for C_1 units is the

1501 methylation of various substrates, such as DNA, RNA, proteins, phospholipids and other

1502 substrates. The shown reactions occur in mitochondria, chloroplasts, and the cytosol,

1503 but may have a preference for a certain subcellular compartment. THF,

1504 tetrahydrofolate; CH_2-THF, 5,10-methylene-THF; 5,10-CH^+-THF, 5,10-methenyl-THF; 5-

1505 CHO-THF, 5-formyl-THF; 10-CHO-THF, 10-formyl-THF; 5-CH_3-THF, 5-methyl-THF; SAM, S-

1506 adenosyl-methionine; SAH, S-adenosyl-homocysteine; fMet-tRNA, N-formylmethionine-

1507 tRNA; GDC, glycine decarboxylase complex; SHMT, serine:hydroxymethyltransferase;

1508 FDF, 10-formyl-THF deformylase; MTHFD, 5,10-methylene-THF dehydrogenase; MTHFC,
1509 5,10-methenyl-THF cyclohydrolase; FTHFC, 5-formyl-THF cyclo-ligase; MTHFR, 5,10-
1510 methylene-THF reductase; MS, methionine synthase; MAT, methionine
1511 adenosyltransferase; MT, methyltransferase; SAHase, S-adenosyl-homocysteine
1512 hydrolase (Figure adapted from Gorelova et al., 2017).
1513

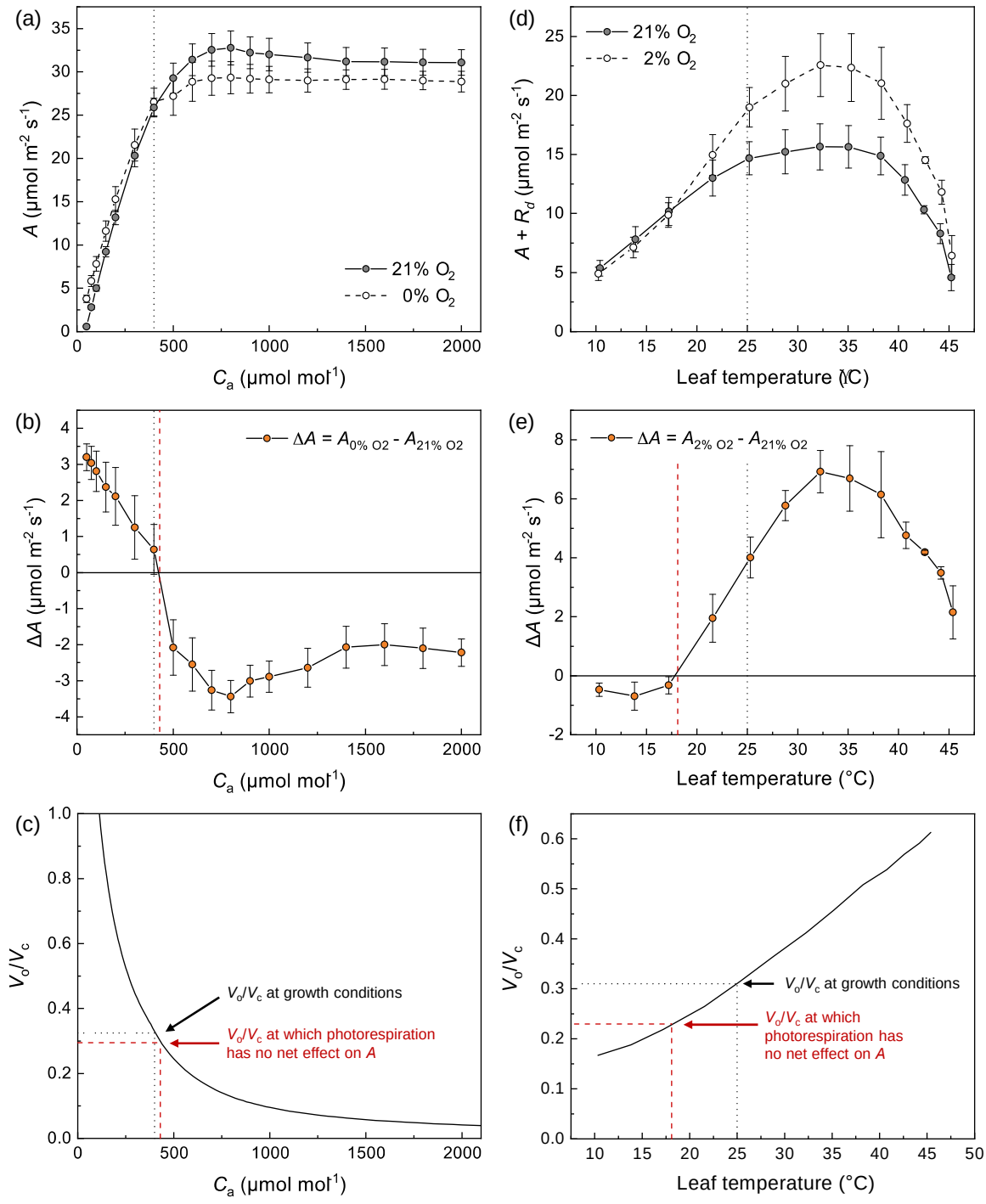

1514 **Figure 5**

1515 **Net effect of photorespiration on CO_2 assimilation rates.** Photorespiration can

1516 transiently be suppressed by decreasing *O* around the leaf. *A* measured during the

1517 instantaneous suppression of the Rubisco oxygenation reaction integrates the

1518 diffusional, biochemical, and physiological effects of photorespiration on net carbon
1519 uptake of the leaf (calculated as ΔA; see Box 1). (a)-(c) The suppression of
1520 photorespiration under varying atmospheric CO_2 concentrations (C_a) for sunflower
1521 (*Helianthus annuus*) leaves fertilized with NO_3^- (data from Busch et al., 2018). (d)-(f) The
1522 suppression of photorespiration under varying leaf temperatures in leaves of sweet
1523 potato (*Ipomoea batatas*; data from Busch and Sage, 2017). Net CO_2 assimilation rates
1524 are measured at oxygen concentrations of 21% and close to 0% (a) or 21% and 2% (b).
1525 The absolute difference between A when photorespiration is present (21% O) and A
1526 when it is absent (0% or 2% O) is displayed in (b) and (e). Note that ΔA in (b) is
1527 estimated from the A/C_a curves rather than A/C_i or A/C_c curves, which ensures all
1528 diffusion resistances, and thus also the effect of the leaf anatomy, is accounted for (see
1529 Box 1 for details). The dotted lines denote ambient conditions (CO_2 concentration: 400
1530 µmol mol^{-1}; growth temperature: 25°C). Red dashed lines denote the CO_2 concentration
1531 and temperature at which the net effect of photorespiration on carbon uptake is zero. In
1532 these examples, at values of C_a above ambient, or leaf temperatures below
1533 approximately 20°C, the net effect of photorespiration on carbon uptake is positive,
1534 meaning that decreasing photorespiration decreases A. At lower C_a, or higher
1535 temperatures, the overall effect of photorespiration is negative and plants would
1536 benefit from decreasing photorespiration. (c) and (f) The ratio V_o/V_c when
1537 photorespiration is present. At ambient C_a, approximately a quarter of Rubisco activity
1538 goes towards oxygenation (c), corresponding to a negligible net effect on carbon uptake
1539 (b). Similarly, at 20°C one fifth of Rubisco activity supports oxygenation (f), again with no

associated costs in net carbon uptake (e). Comparing (b) with (c), and (e) with (f), photorespiration appears to be beneficial in terms of net carbon uptake for a V_o/V_c of up to roughly 0.25.

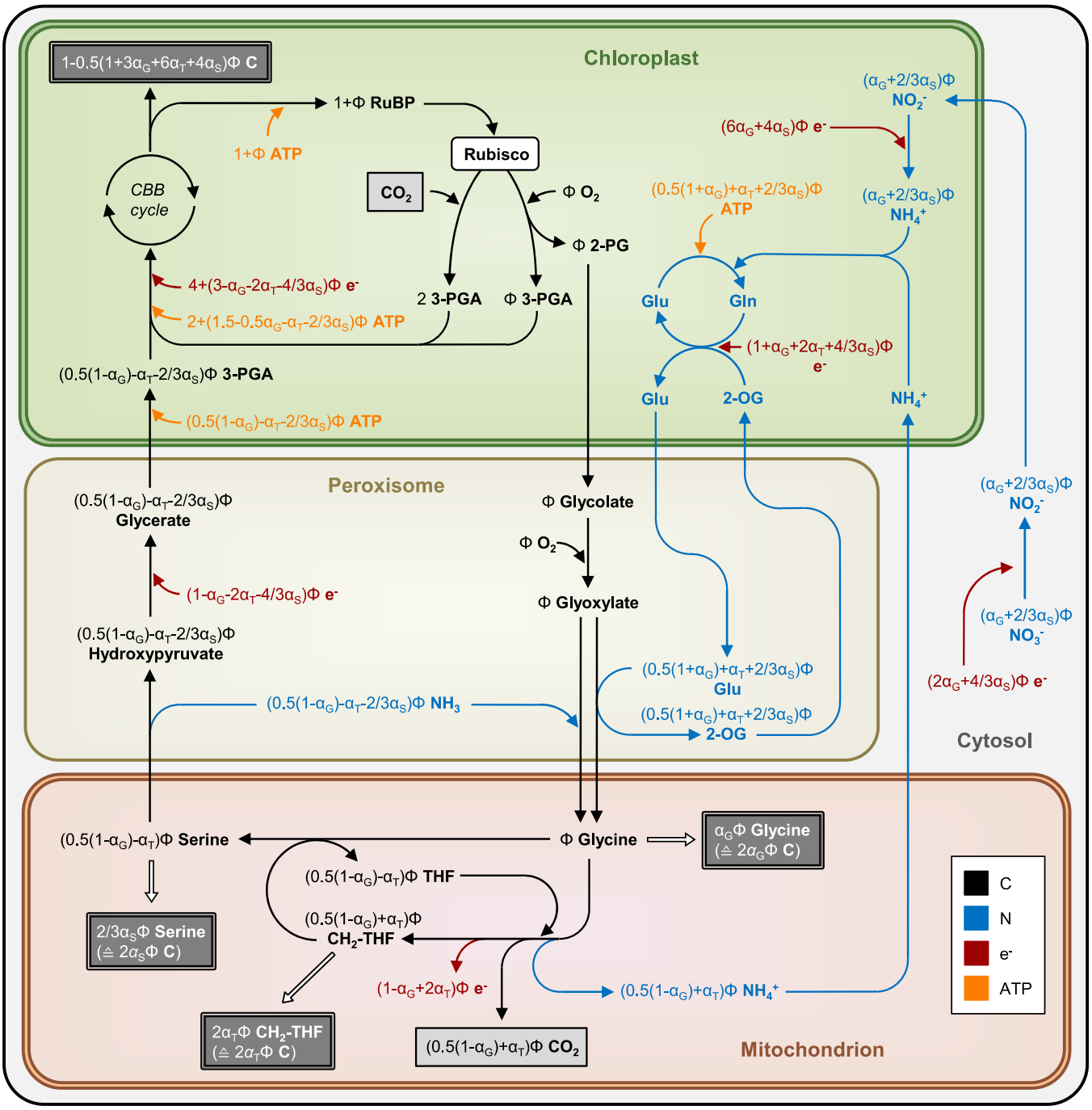

1544

1545 **Supplementary Figure 1**

1546 **Fluxes through the photosynthetic carbon reduction and photorespiratory pathways.**

1547 Outlined are the pathways indicating metabolites (bold font) and stoichiometries

1548 (regular font) of carbon (black) nitrogen (blue) when a proportion of the

photorespiratory carbon leaves the photorespiratory pathway as amino acids and CH_2-THF. Electron and ATP requirements are indicated in red and orange, respectively. The difference between CO_2 taken up by carboxylation and CO_2 released from photorespiration (light gray boxes) equals the sum of the individual sinks for assimilated carbon, indicated by double-bordered gray boxes. The proportion of 2-PG carbon leaving the photorespiratory pathway as glycine is denoted by a_G, that leaving as CH_2-THF by a_T and that leaving as serine by a_S. F represents the ratio of the rates of RuBP oxygenation to that of carboxylation; 3-PGA, 3-phosphoglycerate; 2-PG, 2-phosphoglycolate. All flux magnitudes are scaled in relation to the rate of RuBP carboxylation. Figure adapted from Busch et al. (2018).